

Washington University School of Medicine

Digital Commons@Becker

---

Open Access Publications

---

3-29-2019

## Matching mitochondrial DNA haplotypes for circumventing tissue-specific segregation bias

Jianxin Pan  
*Fudan University*

Li Wang  
*Chinese Academy of Sciences*

Charles Lu  
*Washington University School of Medicine in St. Louis*

Yanming Zhu  
*Fudan University*

Zhunyuan Min  
*Fudan University*

*See next page for additional authors*

Follow this and additional works at: [https://digitalcommons.wustl.edu/open\\_access\\_pubs](https://digitalcommons.wustl.edu/open_access_pubs)

**Please let us know how this document benefits you.**

---

### Recommended Citation

Pan, Jianxin; Wang, Li; Lu, Charles; Zhu, Yanming; Min, Zhunyuan; Dong, Xi; and Sha, Hongying, "Matching mitochondrial DNA haplotypes for circumventing tissue-specific segregation bias." *iScience*. 13, 371 - 379. (2019).

[https://digitalcommons.wustl.edu/open\\_access\\_pubs/9564](https://digitalcommons.wustl.edu/open_access_pubs/9564)

This Open Access Publication is brought to you for free and open access by Digital Commons@Becker. It has been accepted for inclusion in Open Access Publications by an authorized administrator of Digital Commons@Becker. For more information, please contact [vanam@wustl.edu](mailto:vanam@wustl.edu).

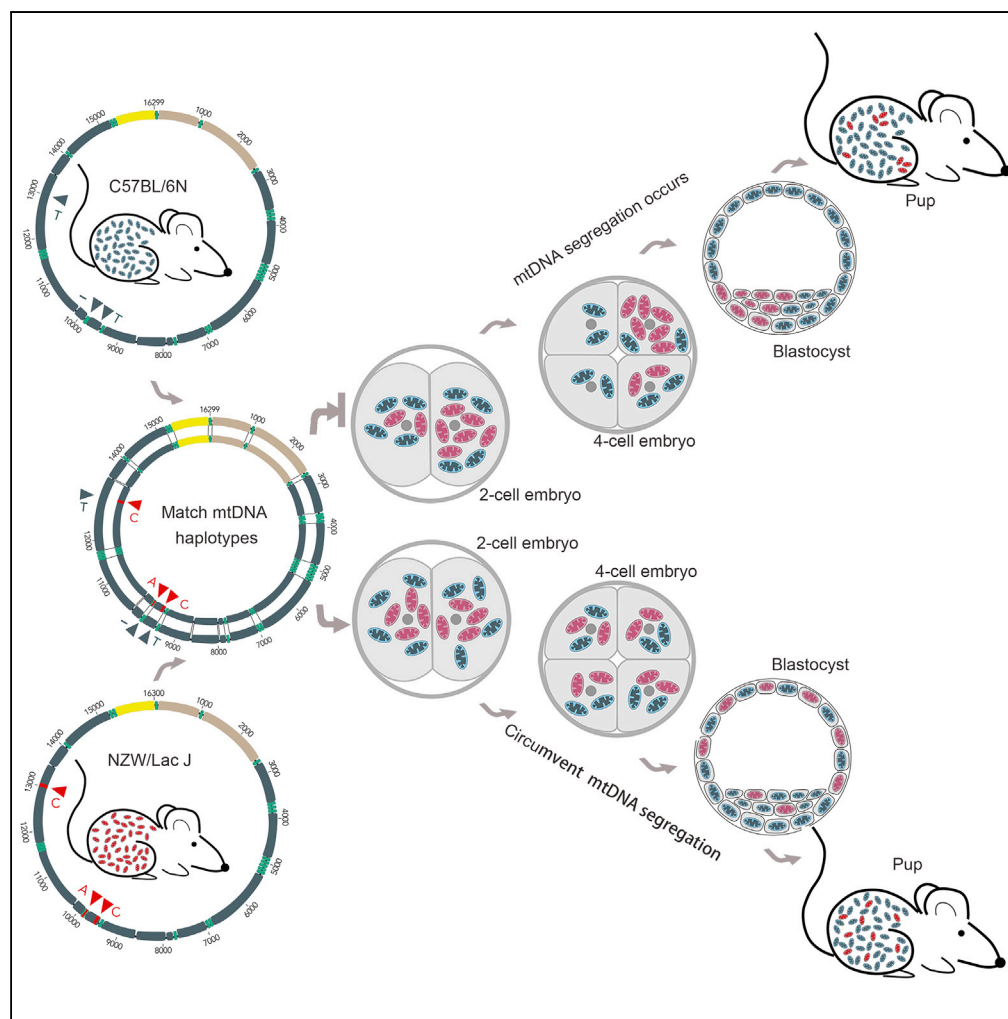
---

**Authors**

Jianxin Pan, Li Wang, Charles Lu, Yanming Zhu, Zhunyu Min, Xi Dong, and Hongying Sha

## Article

# Matching Mitochondrial DNA Haplotypes for Circumventing Tissue-Specific Segregation Bias



Jianxin Pan, Li Wang, Charles Lu, Yanming Zhu, Zhunyuan Min, Xi Dong, Hongying Sha

dong.xj@zs-hospital.sh.cn (X.D.)  
shahongying@fudan.edu.cn (H.S.)

## HIGHLIGHTS

Matching mitochondrial DNA haplotypes make the nucleus treat different mtDNA the same

Similar mtDNA haplotypes prevents tissue-specific segregation bias

Low level of mtDNA heteroplasmy results in uneven inheritance rather than segregation

## Article

# Matching Mitochondrial DNA Haplotypes for Circumventing Tissue-Specific Segregation Bias

Jianxin Pan,<sup>1,4</sup> Li Wang,<sup>2,4</sup> Charles Lu,<sup>1,3</sup> Yanming Zhu,<sup>1</sup> Zhunyuan Min,<sup>1</sup> Xi Dong,<sup>1,\*</sup> and Hongying Sha<sup>1,5,\*</sup>

## SUMMARY

**Mitochondrial DNA (mtDNA) segregation associated with donor-recipient mtDNA mismatch in mitochondria replacement therapy leads to unknown risks. Here, to explore whether matching mtDNA haplotypes contributes to ameliorating segregation, we reproduced various degrees of heteroplasmic mice with three single nucleotide polymorphisms to monitor segregation severity. “Segregation” presented in tissues of heteroplasmic mice containing low-level donor mtDNA heteroplasmy, and disappeared as donor mtDNA heteroplasmy levels ascended. Meanwhile, we found that distribution of donor mtDNA among the blastomeres of preimplantation embryos from the heteroplasmic mice shared the same tendency as that in adult tissues. Statistical analysis showed that no selective replication of donor mtDNA occurred during lifespan. Tracking donor mtDNA distribution showed that uneven distribution of donor mtDNA among embryonic blastomeres gradually became even as donor mtDNA heteroplasmy increased, indicating that the “segregation” in tissues was inherited from the uneven distribution. Our finding suggested that donor-recipient mtDNA matching could circumvent segregation in mitochondria replacement therapy.**

## INTRODUCTION

Mitochondrial replacement has the potential to reduce the transmission of inherited mitochondrial diseases (Wang et al., 2014; Paull et al., 2013; Graven et al., 2010; Tachibana et al., 2009). However, mitochondrial replacement will inevitably result in trace levels of heteroplasmy (Paull et al., 2013; Graven et al., 2010; Tachibana et al., 2009). Although such trace levels of heteroplasmy do not exceed a pathogenic threshold, if the pathogenic maternal mitochondrial DNA (mtDNA) is given a selective advantage, it is possible that it achieves dominance and manifests a pathogenic phenotype through the process of segregation, a common phenomenon in tissues of patients with mitochondrial disease (Frederiksen et al., 2006; Nishizuka et al., 1998). Recent studies of human mitochondrial replacement show sharp drifts of pathogenic mtDNA haplotype on a cellular level (Hyslop et al., 2016; Kang et al., 2016; Yamada et al., 2016), indicating that the nuclear genome preferentially regulates the replication and segregation of the native pathogenic mitochondria. Thus the requirement of a functional match between donor and recipient mtDNA, as well as between the mtDNA and nuclear genome, is of the utmost importance in clinical applications of mitochondria replacement (Latorre-Pellicer et al., 2016; Reinhardt et al., 2013; Sharpley et al., 2012; St John and Campbell, 2010). Previous study suggested that the segregation of donor mtDNA in mitochondria replacement could be alleviated if the donor mtDNA haplotype matches with the recipient mtDNA haplotype (Latorre-Pellicer et al., 2016; Røyrvik et al., 2016).

Obviously, the optimal recipient mitochondria would have the same haplotype as the donor. However, it is impossible to have two identical haplotypes of mtDNA in humans (He et al., 2010). However, the shorter the genetic distance between haplotypes, the less pronounced is the segregation bias. Therefore, exploring haplotype matching between donor and recipient mtDNA is particularly important for eliminating segregation of donor mtDNA. As tissue-specific segregation of different mtDNA genotypes is also common in heteroplasmic mice created from ooplasm or nuclear transfer, various heteroplasmic mice models were used to elucidate the mechanisms for controlling segregation of different mtDNA genotypes (Jokinen et al., 2015; Neupane et al., 2015; Sato et al., 2007; Battersby et al., 2005; Takeda et al., 2000; Jenuth et al., 1997). Among these models, heteroplasmic mice constituted by NZB and C57BL/6N were the dominant heteroplasmic models with 106 single nucleotide polymorphism (SNP) differences. In addition, Burgstaller et al. found highly significant positive correlation between individual tissue-specific segregation and mtDNA genetic distance in specific heteroplasmic mice generated using wild mice in Europe

<sup>1</sup>Reproductive Medicine Center, Zhongshan Hospital, State Key Laboratory of Medical Neurobiology, Institutes of Brain Science, Shanghai Medical College, Fudan University, Shanghai 200032, China

<sup>2</sup>Key Lab of Synthetic Biology of CAS, Shanghai Institute for Biological Sciences, Shanghai Research Center of Biotech., Chinese Academy of Sciences, 500 Caobao Road, Shanghai 200233, China

<sup>3</sup>Washington University in St. Louis, Saint Louis 63110, USA

<sup>4</sup>These authors contributed equally

<sup>5</sup>Lead Contact

\*Correspondence: dong.xi@zs-hospital.sh.cn (X.D.), shahongying@fudan.edu.cn (H.S.)

<https://doi.org/10.1016/j.isci.2019.03.002>





and C57BL/6N, where the wild mice display a spectrum of genetic distance (18, 86, 107, and 416 SNP differences at mtDNA) with C57BL/6N (Burgstaller et al., 2014a). Common segregation present in those heteroplasmic mice indicated that none of the models above underwent haplotype matching, leading to the absence of related progress in segregation.

Here we therefore intend to shorten the distance between the donor and recipient mtDNA haplotypes to explore whether matching mtDNA haplotypes between donor and recipient mtDNA can circumvent the segregation bias toward donor mtDNA in tissues of mitochondria replacement mice (Figures S1A and S1B). We had established a specific model of heteroplasmic mice from NZW/Lac J and B6D2F1 (C57/BL6 $\times$ DBA) using mitochondria replacement from our past study (Wang et al., 2014). The mtDNA genotypes of NZW strain differ from those of C57 strain at only three SNPs, making them ideal models for matching mtDNA haplotypes. To study the effect of matching mtDNA haplotypes on the tissue segregation, we reared offspring of the heteroplasmic mice to test whether matching mtDNA haplotypes between “donor” and “recipient” can circumvent the segregation of donor mtDNA (Figure S1C).

## RESULTS

### Tissue-Specific “Segregation” Gradually Disappeared with the Increase of Donor mtDNA Mean Heteroplasmy in Adult Mice

To explore whether matching mtDNA haplotypes can circumvent the segregation bias, we first sought to test whether the segregation occurred in different tissues from heteroplasmic mice with 3 SNP difference (Table S1), which was derived as described using mitochondria replacement technique (Wang et al., 2014). To avoid the potential impact of heteroplasmy level and trauma from mitochondria replacement manipulation on segregation behavior, heteroplasmic mice from the mitochondria replacement founder were used, which possessed naturally inherited levels of heteroplasmy. Pyrosequencing, which has a 1% detection threshold, 100% sensitivity, and 100% specificity (Hyslop et al., 2016; Wang et al., 2014; Blakely et al., 2013; White et al., 2005) (Figure S2), was adopted to measure the level of donor mtDNA heteroplasmy with primary and second primers (Table S2, also see Transparent Methods). The donor mtDNA heteroplasmy was measured with pyrosequencing in 16 tissues from 37 heteroplasmic mice that were sacrificed as adults (6–8 months old) (Figure 1A). The mean heteroplasmy level of each adult displaces the natural range (from 1.86% to 38.13%) (Figure 1B and Table S3). The heteroplasmic value of 16 tissues showed similar regional distribution ( $p > 0.05$ ) (Figure 1C), which initially indicated that segregation of donor mtDNA does not appear in different tissues of the heteroplasmic mice with 3 SNP difference. After incorporation of different tissues into the corresponding germ layer, it was found that there was no significant difference in donor mtDNA heteroplasmy between the three germ layers ( $p > 0.05$ ) (Figure 1D). Then we compared the distribution of donor mtDNA in individual tissues of each adult mouse using normalized variance ( $V'(h)$ ) calculation as a way to measure the dispersion of donor mtDNA heteroplasmy. A drastic dispersion of donor mtDNA presented in individual tissues of adult mice with lesser than 10% donor mtDNA, evidenced by the greater  $V'(h)$  ( $r = -0.53$ ,  $p < 0.001$ ) (Figure 1E). However, a much narrower distribution with few deviations appeared in individual tissues of adult mice with 10%–20%, or greater than 20%, donor mtDNA, supported by the low  $V'(h)$  (Figure 1E).

### Distribution of Donor mtDNA in the Blastomeres of Preimplantation Embryos Shared the Same Tendency as that in Adult Tissues

It is known that no net replication of mtDNA takes place before embryo implantation. Therefore each subsequent cell division reduces the amount of mtDNA within the daughter cells by about 50% (Carling et al., 2011). Next, to explore whether “segregation” actually occurs at lower levels of heteroplasmy in adult tissues, we observed the distribution of the two different mtDNA genotypes in each blastomere of embryos at 2-cell, 4-cell, and 8-cell stages from the heteroplasmic mice. As the adult tissues of the heteroplasmic mice, embryos at 2-cell, 4-cell, and 8-cell stages maintained a natural distribution value, ranging from 1.95 to 39.63, 1.81 to 54.24, and 2.57 to 51.91, respectively (Figures 2A–2C, Tables S4–S6). Similar to adult tissues, we observed that distribution of donor mtDNA heteroplasmy in each blastomere became less diverse as the mean levels of donor mtDNA heteroplasmy gradually increased in 2-, 4-, and 8-cell embryos, respectively. It was witnessed that  $V'(h)$  values present a negative correlation with the mean heteroplasmy of embryos at 2-, 4-, and 8-cell stages ( $r = -0.45$ ,  $p < 0.05$  for 2-cell stage;  $r = -0.58$ ,  $p < 0.0001$  for 4-cell stage;  $r = -0.48$ ,  $p < 0.005$  for 8-cell stage) (Figure 2D).

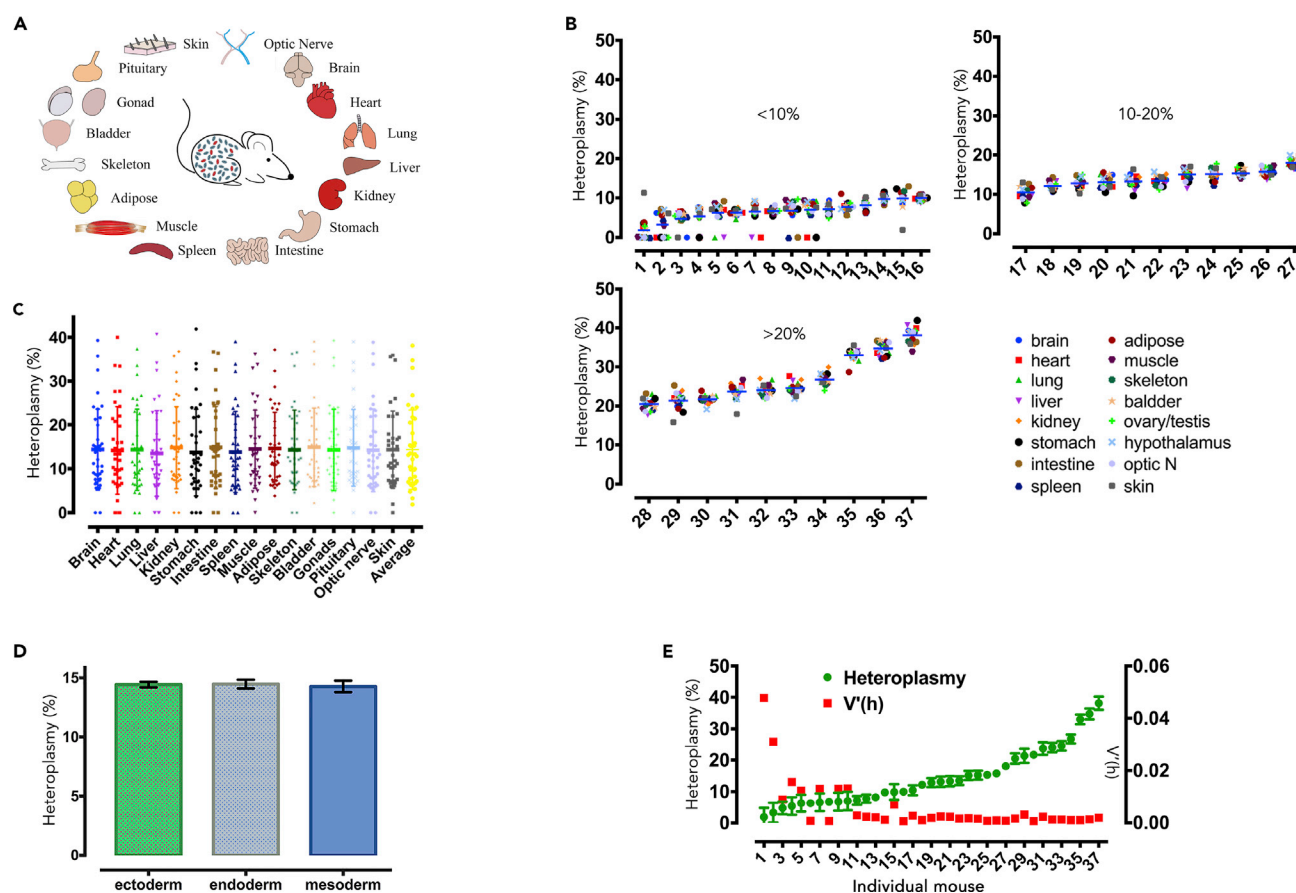


**Figure 1. Tissue-Specific Segregation Disappeared with the Increase of Donor mtDNA Mean Heteroplasmy in Adult Mice**

(A) Schematic model of heteroplasmic mice and dissected tissues in this study.

(B) Heteroplasmy of donor mtDNA in individual tissues from heteroplasmic mice with different heteroplasmic levels.

(C) Comparison of heteroplasmic distribution in 16 tissues from 37 mice ( $p > 0.05$ , Friedman test). Data are represented as scatterplot with mean  $\pm$  SD.

(D) Comparison of mean heteroplasmy levels in the ectoderm, endoderm, and mesoderm ( $p > 0.05$ , Mann-Whitney test). Data are represented as mean  $\pm$  SD.

(E) Negative correlation between heteroplasmic levels (green) and  $V'(h)$  (red) in 16 tissues of each mouse ( $r = -0.53$ ,  $p < 0.001$ , Spearman correlation test). Error bars indicate SD, with the mean value.

See also Table S3.

### No Selective Replication of Donor mtDNA Took Place during the Progressive Cleavage across Developmental Stages

To relate the similar distribution trend of donor mtDNA seen in adult tissues with those in blastomeres of cleaving embryos, we compared the dispersion of donor mtDNA from 2-cell with that from adult stage using several statistical comparison methods. We first observed the spread trends from 2-cell to adult stage. The spread of donor mtDNA heteroplasmy between daughter blastomeres within each embryo, calculated as the heteroplasmic range and  $V'(h)$  values, increased gradually from the 2-cell through the 4-cell to 8-cell groups ( $p < 0.05$ ) (Figures 3A–3D). These phenomena are consistent with recent studies' findings, which showed increasing cell-to-cell heteroplasmy variability through early embryonic cleavages (Lee et al., 2012; Johnston et al., 2015; Johnston and Jones, 2015, 2016). However, the spread trend returned to the original level as that of 2-cell embryos as development progresses to adult stage (Figures 3A–3D). Then we further found that adult tissues share a similar distribution of heteroplasmy with early embryos at 2-, 4-, and 8-cell stages ( $p > 0.05$ ), calculated as mean heteroplasmy (Figure 3E), frequency distribution (Figure 3F), and cumulative probability distribution (Figure 3G). Thus, from the spread trends and the distribution, it can be deduced that the distribution of donor mtDNA in adult tissues depends on the distribution present in early embryos, suggesting that no selective replication of donor mtDNA took place during the progressive cleavage from the 2- to 4- to 8-cell stages extending to adult.

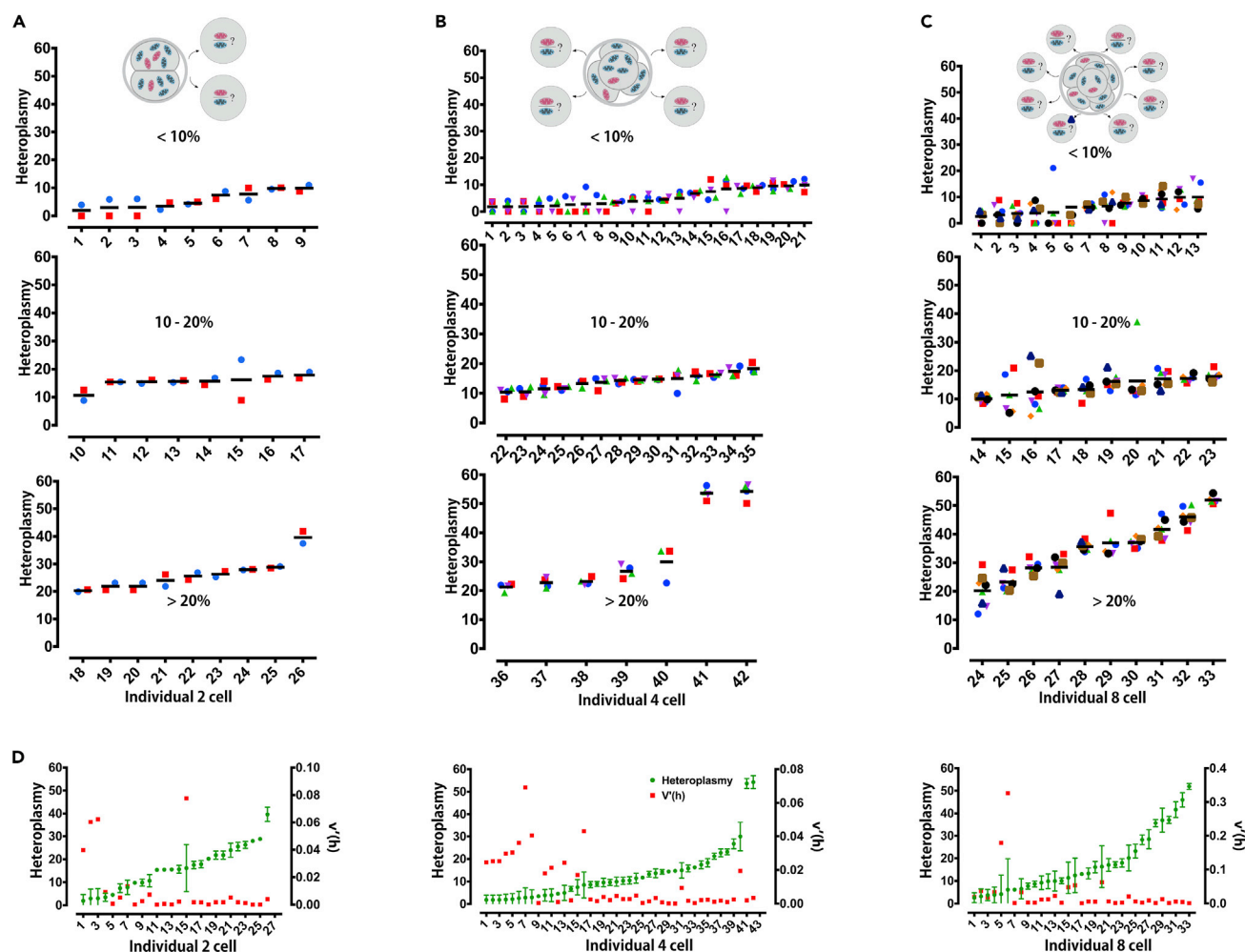


**Figure 2. Distribution of Donor mtDNA in the Blastomeres of Pre-implantation Embryos Shared the Same Tendency as that in Adult Tissues**

(A) Schematic model of embryos and dissected blastomeres of embryos at 2-cell stage. Heteroplasmy distribution of donor mtDNA in blastomeres of embryos at 2-cell stage from heteroplasmic mice.

(B) Schematic model of embryos and dissected blastomeres of embryos at 4-cell stage. Heteroplasmy distribution of donor mtDNA in blastomeres of embryos at 4-cell stage from heteroplasmic mice.

(C) Schematic model of embryos and dissected blastomeres of embryos at 8-cell stage. Heteroplasmy distribution of donor mtDNA in blastomeres of embryos at 8-cell stage from heteroplasmic mice.

(D) Negative correlation between donor mtDNA heteroplasmy (green) and  $V'(h)$  (red) values in blastomeres of embryos at 2, 4, and 8-cell stage ( $r = -0.45$ ,  $p < 0.05$  for 2-cell stage;  $r = -0.58$ ,  $p < 0.0001$  for 4-cell stage;  $r = -0.48$ ,  $p < 0.005$  for 8-cell stage. Spearman correlation test).

Error bars indicate SD, with the mean value. See also Tables S4–S6.

### Tracking Donor mtDNA Distribution Exhibited that Low Level of Donor mtDNA Heteroplasmy Resulted in Its Uneven Inheritance during Early Embryonic Cleavage

To explore why donor mtDNA deviation occur in tissues and blastomeres in the <10% group, we generated heteroplasmic oocytes to observe the distribution of donor mtDNA via spindle-chromosome complex transfer (spindle transfer) (Figure 4A) (Wang et al., 2014). Briefly, the donor mitochondria were labeled with 250 nM MitoTracker Red. Then spindle transfer was performed between the stained oocytes (donor) and unstained oocytes (recipient) (Figures 4A and 4B and Video S1). Differing amounts of donor mtDNA were fused into an enucleated recipient oocyte, resulting in varying levels of heteroplasmy (<10% and >10%; here we only use >10% as past results showed no significant difference between the 10% to 20% and the >20% groups). The levels of heteroplasmy were calculated from the volume ratio (on average 10%:90%) by measuring the diameters of karyoplasts (carrying donor mtDNA). After the oocytes were fertilized *in vitro* and development proceeded, red mitochondria

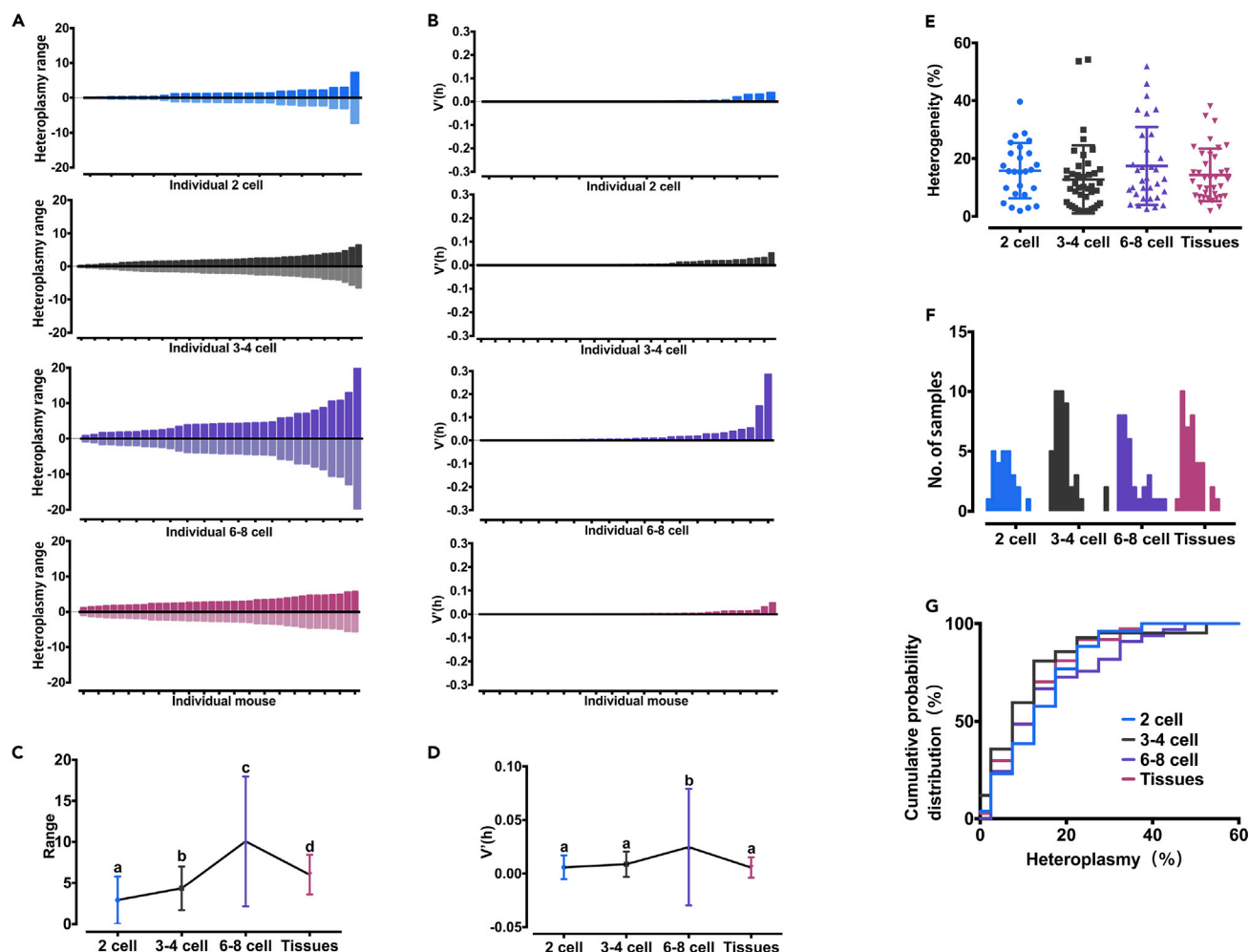


**Figure 3. No selective replication of donor mtDNA took place during the progressive cleavage across developmental stages**

(A and B) (A) Spread of donor mtDNA heteroplasmy from embryonic blastomere to adult tissue expressed by heteroplasmy range (maximum or minimum heteroplasmy value minus the mean median of heteroplasmy value). The mean median is defined as half of the sum of maximum and minimum values. Light bar = maximum – median = maximum –  $\frac{\text{maximum} + \text{minimum}}{2}$  =  $\frac{\text{maximum} - \text{minimum}}{2}$ ; dark bar = minimum – median = minimum –  $\frac{\text{maximum} + \text{minimum}}{2}$  =  $-\frac{\text{maximum} - \text{minimum}}{2}$  (B)  $V'(h)$  values of embryonic blastomeres and adult tissue.

(C) Comparison of the spread ranges among embryos at 2-, 4-, and 8-cell stage and adults. Data are represented as mean  $\pm$  SD.

(D) Comparison of  $V'(h)$  values among embryos at 2-, 4-, and 8-cell stage and adults. Different letters indicate p values < 0.05 (Mann-Whitney test); error bars indicate SD. See also Tables S3–S6.

(E) Comparison of mean heteroplasmy values of embryos at 2-, 4-, and 8-cell stage and adult tissues (p > 0.05, Mann-Whitney test). Data are represented as scatterplot with mean  $\pm$  SD.

(F) Frequency histogram of the donor mtDNA heteroplasmy of embryos at 2-, 4-, and 8-cell stage and adult tissues.

(G) Cumulative probability distribution functions for the heteroplasmy of embryos at 2-, 4-, and 8-cell stage and adult tissues. (p > 0.05, Kolmogorov-Smirnov test).

See also Tables S3–S6.

distribution was monitored in individual blastomeres of embryos at the 2-, 4-, and 8-cell stages and the blastocyst. A distinct correlation was observed between the distribution of donor mitochondria and the level of heteroplasmy. For <10% group, uneven and even configurations of red mitochondria distribution were found in the preimplantation embryos from 2-cell to blastocyst stage. In the uneven group, the number of red mitochondria in each blastomere varied significantly under confocal microscope, with no red mitochondria in several of the blastomeres (Figures 4B and S3–S6). By contrast, almost equal numbers of red granules were distributed in each blastomere in the even group (Figures 4B and S3–S6). However, in cells with higher levels of heteroplasmy (>10%), we observed only even distribution of stained mitochondria, with cells portraying close to equal levels of heteroplasmy (Figures 4B

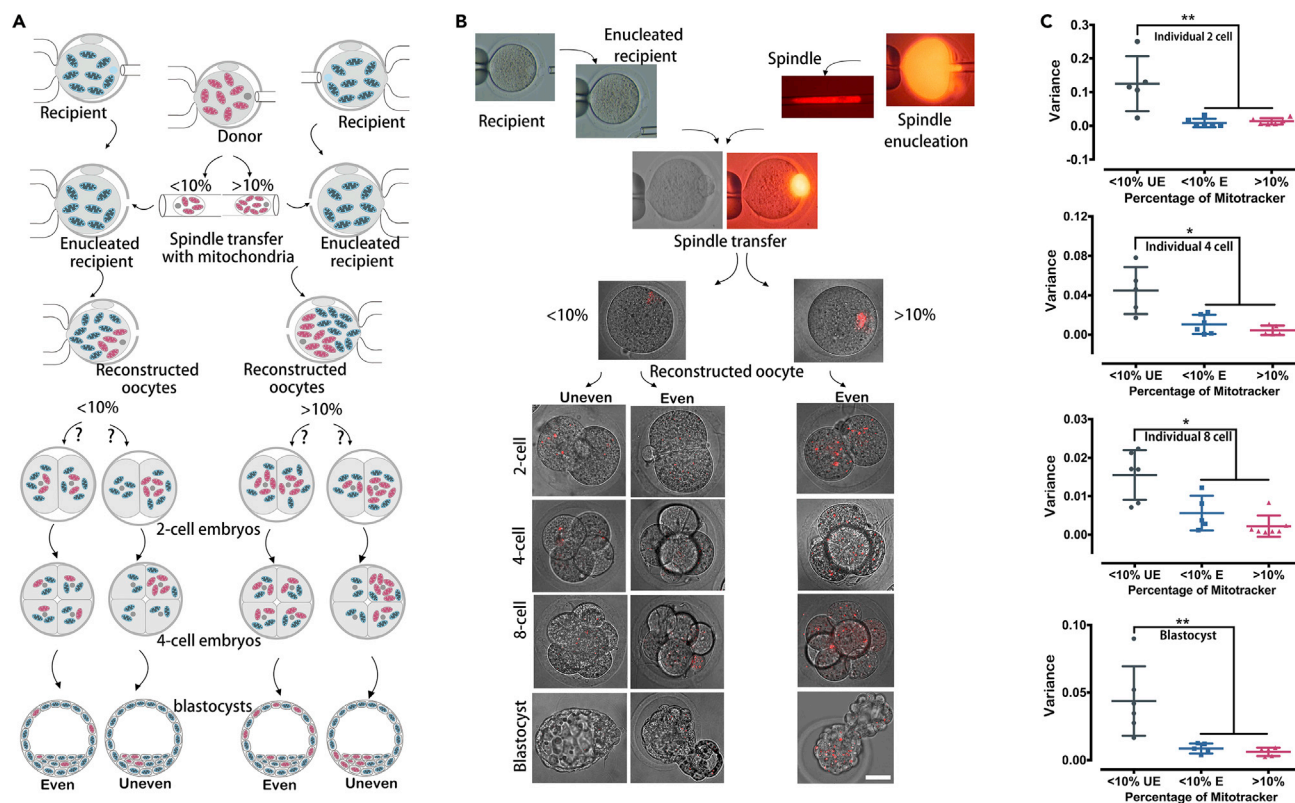


**Figure 4. Tracking Donor mtDNA Distribution in Pre-implantation Embryos Exhibited that Low Level of Heteroplasmy Led to Its Uneven Inheritance during Cleavage**

(A) Schematic model showing how differing amounts of donor mitochondria were transferred into the recipient oocytes, resulting in the formation of the <10% heteroplasmy group and the >10% heteroplasmy group (here we only use >10% as past results showed no significant difference between the 10%–20% and >20% group). Depicts the two possible outcomes for each group: even distribution or uneven distribution.

(B) The spindle transfer manipulation that resulted into the two groups of differing heteroplasmy (images were taken with Nikon TE, 2000 microscope, 40X); the two separate groups of heteroplasmic oocytes with different heteroplasmy of donor mtDNA; the final outcome of the two groups, with the <10% group displaying both even and uneven distributions of donor mtDNA in pre-implantation development (images were taken with Leica confocal scanning microscope, 63X). The images of 2-cell in <10% uneven and >10% even, and blastocyst in <10% uneven and <10% even were also used for measuring fluorescence intensity in Figures S3 and S6, respectively.

(C) Statistical comparison of MitoTracker Red distribution in each blastomere of embryos at 2-, 4-, and 8-cell stage and blastocysts. UE, uneven; E, even. Data are represented as scatterplot with mean  $\pm$  SD. Asterisks indicated significant differences (\* $p$  < 0.05, \*\* $p$  < 0.01, Mann-Whitney test). Scale bar, 40  $\mu$ m.

See also Video S1, Figures S3–S6 and Tables S7–S10.

and S3–S6). Furthermore, statistical comparison found that there were significant differences between <10% uneven and <10% even or >10% groups for donor mtDNA distribution in each blastomere of embryos at 2-, 4-, and 8-cell stages and blastocysts (Figures 4C and S3–S6 and Tables S7–S10). On the contrary, there were no obvious differences between <10% even and >10% groups for the distribution in each blastomere of embryos at 2-, 4-, and 8-cell stages and blastocysts (Figures 4C and S3–S6 and Tables S7–S10). This suggests that disproportionate variance increase can arise from partitioning noise with low mitochondrial volumes.

## DISCUSSION

As we know, segregation of mutant mtDNA is a universal event during individual development (Burgstaller et al., 2014b). The coexistence of two kinds of mitochondria and its mtDNA may have fatal consequences for the development of offspring (Schon et al., 2012). Mitochondrial replacement technology will inevitably lead to the coexistence of two kinds of mitochondria and mtDNA, so the public has been worried about the potential safety risks since its conception. This study demonstrated that matching the haplotypes of the donor and recipient mtDNA has the potential to circumvent segregation bias and prevent the occurrence of mitochondrial diseases.



When heteroplasmic values are close to the detection limit, technical variability will likely be mixed in with the biological variability and may contribute to “segregation” as well. However, the spread trend of mtDNA heteroplasmy in preimplantation embryo was consistent with recent studies (Johnston et al., 2015; Lee et al., 2012), suggesting that heteroplasmic values from pyrosequencing are reliable in our study. Our results showed that uneven inheritance donor mtDNA in embryonic blastomeres rather than selective replication of donor mtDNA causes the “segregation” in adult tissues of heteroplasmic mice with low level of heteroplasmy. The spread trend of donor mtDNA heteroplasmy and V(h) values increases from 2-cell, through 3- to 4-cell, to 6- to 8-cell blastomeres, evidenced by how the spread trend of 8-cell is greater in turn than that of 4-cell and 2-cell blastomeres. This phenomenon is consistent with the results of Johnston et al. and Lee et al. studies (Johnston et al., 2015; Lee et al., 2012). Recent studies showed that mitochondrial concentration is controlled in the stochastic partition between cell division (Das Neves et al., 2010; Jajoo et al., 2016). Thus the spread trend could be attributed to how donor mitochondria are randomly assigned into two daughter blastomeres during mitosis of preimplantation embryos, resulting in much higher uneven inheritance of mtDNA in each blastomere when cleavage frequency increased, due to how they are stochastically partitioned during cell division. However, the spread trend in adult tissues almost resumes the initial spread range of the first embryonic cleavage in this study (Figures 3A–3D). As development progressed to adult stage, each tissue may be developed from more than one blastomere of an embryo at 8-cell stage, thus leading to the spread trend initialization, which indicated that no selective replication of donor mtDNA took place during the progressive cleavage across developmental stages.

Burgstaller et al. found that mtDNA segregation in heteroplasmic tissues is common *in vivo* and may be modulated by haplotype differences (Burgstaller et al., 2014a). Based upon their data (See Methods-Mathematical Analysis section), we created a mathematical model and formula that describes the relationship between the proliferation rate of donor mtDNA and genetic distance. From the formula we can deduce that when genetic distance ( $d$ ) of haplotype differences is equal to or less than 9 SNPs, the expected level of segregation, albeit with substantial uncertainty, drops to zero (Figure S7). Thus, in our study, no segregation is present in tissue of heteroplasmic mice containing two mtDNA genotypes of NZW strain and C57 strain, as the mtDNA genotypes differ at only three SNPs. As mtDNA segregation is controlled by the nuclear genome (Agaronyan et al., 2015; Battersby et al., 2003), our results suggest that haplotype matching matches foreign mitochondrial and nuclear DNA as well, so that the nucleus treats similar mtDNA sequence the same, thus preventing segregation.

As we know, mtDNA point mutation causes a variety of different phenotypes in humans. The effect of point mutations on segregation in different tissues during lifetime is still enigmatic. Segregation of some mtDNA mutations, such as 8993T > G, yield no tissue segregation (White et al., 1999), whereas for others, such as 3243A > G, segregation varies drastically among tissues (Frederiksen et al., 2006). The latter seems to violate our results and speculation from Burgstaller’s data, in which differences less than 9 SNPs could circumvent segregation of mutant mitochondria (Figure S7). Owing to a rapid mutation rate over the human lifetime, a number of novel mtDNA mutations, which constitutes mtDNA polymorphisms, were detected in both pathogenic mtDNA carriers’ oocytes (Kang et al., 2016). Owing to how genetic distance between two random selected people will differ at 100 SNPs (Røyrvik et al., 2016), previous studies found that polymorphisms can grant a replicative advantage (Burgstaller et al., 2014b; Kang et al., 2016). It has been demonstrated that some mtDNA point mutations, such as 3394C variant, may either be deleterious or beneficial depending on its haplogroup and environmental context (Ji et al., 2012), suggesting the segregation of point mutations associated with the polymorphisms. We hypothesize that original polymorphisms and novel variations may interact with pathogenic point mutation to constitute a network with nuclear DNA to regulate mutant and non-mutant mtDNA proliferation. Thus, multiple factors should be combined and taken into account for the point mutations as well as other mutants on segregation in further study.

In summary, mitochondrial segregation inevitably occurs in offspring from mitochondrial replacement manipulation if no haplotype matching has been conducted. This study indicates that genetic similarity between donor and recipient mtDNA has the potential to circumvent the segregation bias toward pathogenic maternal mtDNA in tissues of mitochondria replacement offspring. Thus our results recommend that mtDNA haplotype matching should be undertaken between the donor and recipient, as it could “fool” the nucleus into treating the donated mtDNA and the native pathogenic mtDNA the same, thereby eliminating any proliferative advantage, and circumvent any segregation bias and prevent the onset of mitochondrial diseases.

## Limitations of the Study

Although this study has demonstrated that matching mtDNA haplotypes could circumvent the tissue segregation of mutant mitochondria in heteroplasmic mice with 3 SNP difference, more spectra (such as 3–18 SNPs) of mitochondrial genetic differences between two kinds of mice should be conducted to clearly address the minimum distance that can circumvent tissue segregation. Furthermore, screening key SNP loci or regulatory networks, which is associated with mtDNA replication and proliferation in nuclear and mtDNA sequences, may make it easier to find a suitable recipient donation and prevent the occurrence of mitochondrial diseases.

## METHODS

All methods can be found in the accompanying [Transparent Methods supplemental file](#).

## SUPPLEMENTAL INFORMATION

Supplemental Information can be found online at <https://doi.org/10.1016/j.isci.2019.03.002>.

## ACKNOWLEDGMENTS

This study was supported by grants from National Natural Science Foundation of China (81471512 and 31871506 to H.S.).

## AUTHOR CONTRIBUTIONS

H.S. and X.D. supervised and designed the experiments. H.S. and J.P. manipulated mitochondrial donation. J.P. and C.L. performed staining and confocal analysis. L.W. detected heteroplasmy level of samples. Y.Z. did data statistics. Z.M. supervised mice. H.S., C.L., and J.P. prepared the figures and wrote the manuscript.

## DECLARATION OF INTERESTS

The authors declare no competing interests.

Received: October 22, 2018

Revised: January 13, 2019

Accepted: March 1, 2019

Published: March 29, 2019

## REFERENCES

- Agaronyan, K., Morozov, Y.I., Anikin, M., and Temiakov, D. (2015). Replication-transcription switch in human mitochondria. *Science* 347, 548–551.
- Battersby, B.J., Loreda-Osti, J.C., and Shoubridge, E.A. (2003). Nuclear genetic control of mitochondrial DNA segregation. *Nat. Genet.* 33, 183–186.
- Battersby, B.J., Redpath, M.E., and Shoubridge, E.A. (2005). Mitochondrial DNA segregation in hematopoietic lineages does not depend on MHC presentation of mitochondrially encoded peptides. *Hum. Mol. Genet.* 14, 2587–2594.
- Blakely, E.L., Yarham, J.W., Alston, C.L., Craig, K., Poulton, J., Brierley, C., Park, S.M., Dean, A., Xuereb, J.H., Anderson, K.N., et al. (2013). Pathogenic mitochondrial tRNA point mutations: nine novel mutations affirm their importance as a cause of mitochondrial disease. *Hum. Mutat.* 34, 1260–1268.
- Burgstaller, J.P., Johnston, I.G., Jones, N.S., Albrechtová, J., Kolbe, T., Vogl, C., Futschik, A., Mayrhofer, C., Klein, D., Sabitzer, S., et al. (2014a). mtDNA segregation in heteroplasmic tissues is common in vivo and modulated by haplotype differences and developmental stage. *Cell Rep.* 7, 2031–2041.
- Burgstaller, J.P., Johnston, I.G., and Poulton, J. (2014b). Mitochondrial DNA disease and developmental implications for reproductive strategies. *Mol. Hum. Reprod.* 21, 11–22.
- Carling, P.J., Cree, L.M., and Chinnery, P.F. (2011). The implications of mitochondrial DNA copy number regulation during embryogenesis. *Mitochondrion* 11, 686–692.
- Das Neves, R.P., Jones, N.S., Andreu, L., Gupta, R., Enver, T., and Iborra, F.J. (2010). Connecting variability in global transcription rate to mitochondrial variability. *PLoS Biol.* 8, e1000560.
- Frederiksen, A.L., Andersen, P.H., Kyvik, K.O., Jeppesen, T.D., Vissing, J., and Schwartz, M. (2006). Tissue specific distribution of the 3243A->G mtDNA mutation. *J. Med. Genet.* 43, 671–677.
- Graven, L., Tuppen, H.A., Greggains, G.D., Harbottle, S.J., Murphy, J.L., Cree, L.M., Murdoch, A.P., Chinnery, P.F., Taylor, R.W., Lightowlers, R.N., et al. (2010). Pronuclear transfer in human embryos to prevent transmission of mitochondrial DNA disease. *Nature* 465, 82–85.
- He, Y., Wu, J., Dressman, D.C., Iacobuzio-Donahue, C., Markowitz, S.D., Velculescu, V.E., Diaz, L.A., Jr., Kinzler, K.W., Vogelstein, B., and Papadopoulos, N. (2010). Heteroplasmic mitochondrial DNA mutations in normal and tumour cells. *Nature* 464, 610–614.
- Hyslop, L.A., Blakeley, P., Craven, L., Richardson, J., Fogarty, N.M., Fragouli, E., Lamb, M., Wamaitha, S.E., Prathalingam, N., Zhang, Q., et al. (2016). Towards clinical application of pronuclear transfer to prevent mitochondrial DNA disease. *Nature* 534, 383–386.
- Jajoo, R., Jung, Y., Huh, D., Viana, M.P., Rafelski, S.M., Springer, M., and Paulsson, J. (2016). Accurate concentration control of mitochondria and nucleoids. *Science* 351, 169–172.
- Jenuth, J.P., Peterson, A.C., and Shoubridge, E.A. (1997). Tissue-specific selection for different mtDNA genotypes in heteroplasmic mice. *Nat. Genet.* 16, 93–95.

Ji, F., Sharpley, M.S., Derbeneva, O., Alves, L.S., Qian, P., Wang, Y., Chalkia, D., Lvova, M., Xu, J., Yao, W., et al. (2012). Mitochondrial DNA variant associated with Leber hereditary optic neuropathy and high-altitude Tibetans. *Proc. Natl. Acad. Sci. U S A* 109, 7391–7396.

Johnston, I.G., and Jones, N.S. (2015). Closed-form stochastic solutions for non-equilibrium dynamics and inheritance of cellular components over many cell divisions. *Proc. Math. Phys. Eng. Sci.* 471, 20150050.

Johnston, I.G., and Jones, N.S. (2016). Evolution of cell-to-cell variability in stochastic, controlled, heteroplasmic mtDNA populations. *Am. J. Hum. Genet.* 99, 1150–1162.

Johnston, I.G., Burgstaller, J.P., Havlicek, V., Kolbe, T., Rülcke, T., Brem, G., Poulton, J., and Jones, N.S. (2015). Stochastic modelling, bayesian inference, and new in vivo measurements elucidate the debated mtDNA bottleneck mechanism. *Elife* 4, e07464.

Jokinen, R., Marttinen, P., Stewart, J.B., Dear, T.N., and Battersby, B.J. (2015). Tissue-specific modulation of mitochondrial DNA segregation by a defect in mitochondrial division. *Hum. Mol. Genet.* 25, 706–714.

Kang, E., Wu, J., Gutierrez, N.M., Koski, A., Tippner-Hedges, R., Agaronyan, K., Platero-Luengo, A., Martinez-Redondo, P., Ma, H., Lee, Y., et al. (2016). Mitochondrial replacement in human oocytes carrying pathogenic mitochondrial DNA mutations. *Nature* 540, 270–275.

Latorre-Pellicer, A., Moreno-Loshuertos, R., Lechuga-Vieco, A.V., Sánchez-Cabo, F., Torroja, C., Acín-Pérez, R., Calvo, E., Aix, E., González-Guerra, A., Logan, A., et al. (2016). Mitochondrial and nuclear DNA matching shapes metabolism and healthy ageing. *Nature* 535, 561–565.

Lee, H.S., Ma, H., Juanes, R.C., Tachibana, M., Sparman, M., Woodward, J., Ramsey, C., Xu, J.,

Kang, E.J., Amato, P., et al. (2012). Rapid mitochondrial DNA segregation in primate preimplantation embryos precedes somatic and germline bottleneck. *Cell. Rep.* 1, 506–515.

Neupane, J., Ghimire, S., Vandewoestyne, M., Lu, Y., Gerris, J., Van Coster, R., Deroo, T., Deforce, D., Vansteelandt, S., De Sutter, P., et al. (2015). Cellular heterogeneity in the level of mtDNA heteroplasmy in mouse embryonic stem cells. *Cell Rep.* 13, 1304–1309.

Nishizuka, S., Tamura, G., Goto, Y., Murayama, K., Konno, T., Hakozaiki, M., Nonaka, I., Tohgi, H., and Satodate, R. (1998). Tissue-specific involvement of multiple mitochondrial DNA deletions in familial mitochondrial myopathy. *Biochem. Biophys. Res. Commun.* 247, 24–27.

Paull, D., Emmanuele, V., Weiss, K.A., Treff, N., Stewart, L., Hua, H., Zimmer, M., Kahler, D.J., Goland, R.S., Noggle, S.A., et al. (2013). Nuclear genome transfer in human oocytes eliminates mitochondrial DNA variants. *Nature* 493, 632–637.

Reinhardt, K., Dowling, D.K., and Morrow, E.H. (2013). Mitochondrial replacement, evolution, and the clinic. *Science* 341, 1345–1346.

Røyrvik, E.C., Burgstaller, J.P., and Johnston, I.G. (2016). mtDNA diversity in human populations highlights the merit of haplotype matching in gene therapies. *Mol. Hum. Reprod.* 22, 809–817.

Sato, A., Nakada, K., Shitara, H., Kasahara, A., Yonekawa, H., and Hayashi, J. (2007). Deletion-mutant mtDNA increases in somatic tissues but decreases in female germ cells with age. *Genetics* 177, 2031–2037.

Schon, E.A., DiMauro, S., and Hirano, M. (2012). Human mitochondrial DNA: roles of inherited and somatic mutations. *Nat. Rev. Genet.* 13, 878.

Sharpley, M.S., Marciniak, C., Eckel-Mahan, K., McManus, M., Crimi, M., Waymire, K., Lin, C.S., Masubuchi, S., Friend, N., Koike, M., et al. (2012).

Heteroplasmy of mouse mtDNA is genetically unstable and results in altered behavior and cognition. *Cell* 151, 333–343.

St John, J.C., and Campbell, K.H. (2010). The battle to prevent the transmission of mitochondrial DNA disease: is karyoplast transfer the answer? *Gene Ther.* 17, 147–149.

Tachibana, M., Sparman, M., Sritanadomchai, H., Ma, H., Clepper, L., Woodward, J., Li, Y., Ramsey, C., Kolotushkina, O., and Mitalipov, S. (2009). Mitochondrial gene replacement in primate offspring and embryonic stem cells. *Nature* 461, 367–372.

Takeda, K., Takahashi, S., Onishi, A., Hanada, H., and Imai, H. (2000). Replicative advantage and tissue-specific segregation of RR mitochondrial DNA between C57bl/6 and RR heteroplasmic mice. *Genetics* 155, 777–783.

Wang, T., Sha, H., Ji, D., Zhang, H.L., Chen, D., Cao, Y., and Zhu, J. (2014). Polar body genome transfer for preventing the transmission of inherited mitochondrial diseases. *Cell* 157, 1591–1604.

White, H.E., Durston, V.J., Seller, A., Fratter, C., Harvey, J.F., and Cross, N.C. (2005). Accurate detection and quantitation of heteroplasmic mitochondrial point mutations by pyrosequencing. *Genet. Test* 9, 190–199.

White, S.L., Collins, V.R., Wolfe, R., Cleary, M.A., Shanske, S., DiMauro, S., Dahl, H.H., and Thorburn, D.R. (1999). Genetic counseling and prenatal diagnosis for the mitochondrial DNA mutations at nucleotide 8993. *Am. J. Hum. Genet.* 65, 474–482.

Yamada, M., Emmanuele, V., Sanchez-Quintero, M.J., Sun, B., Lallo, G., Paull, D., Zimmer, M., Pagett, S., Prosser, R.W., Sauer, M.V., et al. (2016). Genetic drift can compromise mitochondrial replacement by nuclear transfer in human oocytes. *Cell Stem Cell* 18, 749–754.



**ISCI, Volume 13**

## **Supplemental Information**

### **Matching Mitochondrial DNA Haplotypes for Circumventing Tissue-Specific Segregation Bias**

**Jianxin Pan, Li Wang, Charles Lu, Yanming Zhu, Zhunyu Min, Xi Dong, and Hongying Sha**

## Supplemental Figures and Legends

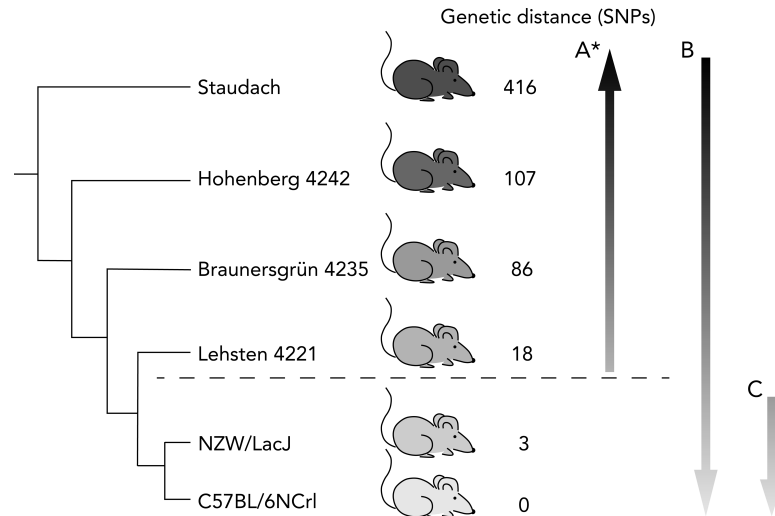


**Figure S1. Schematic charts of this study hypothesis: Phylogenetic tree hypothesizes the correlation between tissue segregation of mtDNA and mitochondrial genetic distance,** Related to Figure 1.

(A) Segregation increases with the genetic distance between "donor" and "recipient" mtDNA haplotypes. \* Referred to Burgstaller et al. Cell Reports 7, 2031–2041, 2014. (B) Hypothesis of this study: shortening genetic distance between "donor" and "recipient" can circumvent the segregation of pathogenic maternal mtDNA. (C) Experiments of this study.

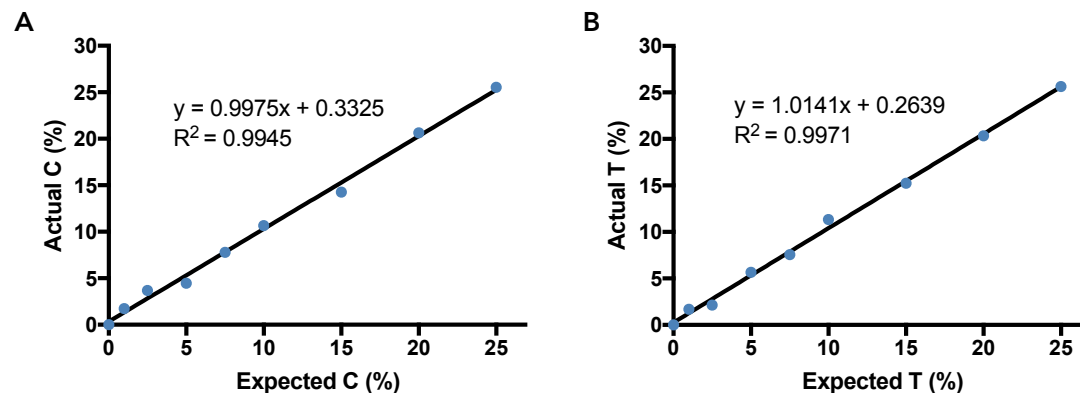


**Figure S2. Standard curves for the pyrosequencing assay, Related to Figures 1, 2 and Transparent Methods**

(A) Linear relationship between the actual heteroplasmy values and expected heteroplasmy values of SNP "C". (B) Linear relationship between the actual heteroplasmy values and expected heteroplasmy values of SNP "T". The lowest reliable level of heteroplasmy detection is 1%. Each data point indicates the mean of triplicate samples.

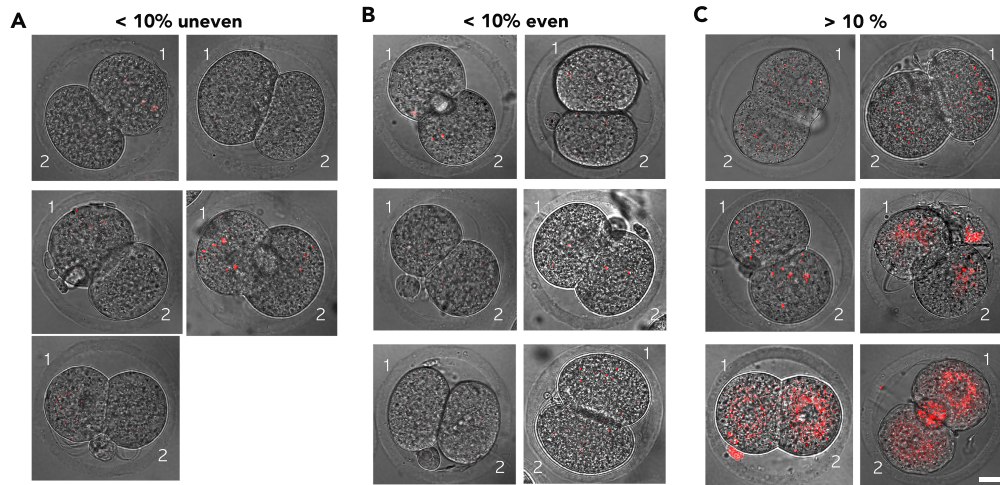


**Figure S3. Tracking donor mtDNA distribution in embryos at 2-cell stage,** Related to Figure 4 (A) Uneven distribution of donor mtDNA in embryos at 2-cell stage from heteroplasmic oocytes with <10% donor mtDNA. (B) Even distribution of donor mtDNA in embryos at 2-cell stage from heteroplasmic oocytes with <10% donor mtDNA. (C) Even distribution of donor mtDNA in embryos at 2-cell stage from heteroplasmic oocytes with >10% donor mtDNA. The fourth image in (A) and the third image in (C) (count by row) was also presented in Figure 4B to demonstrate the living cell staining experiment. Scale bar, 40  $\mu$ m.

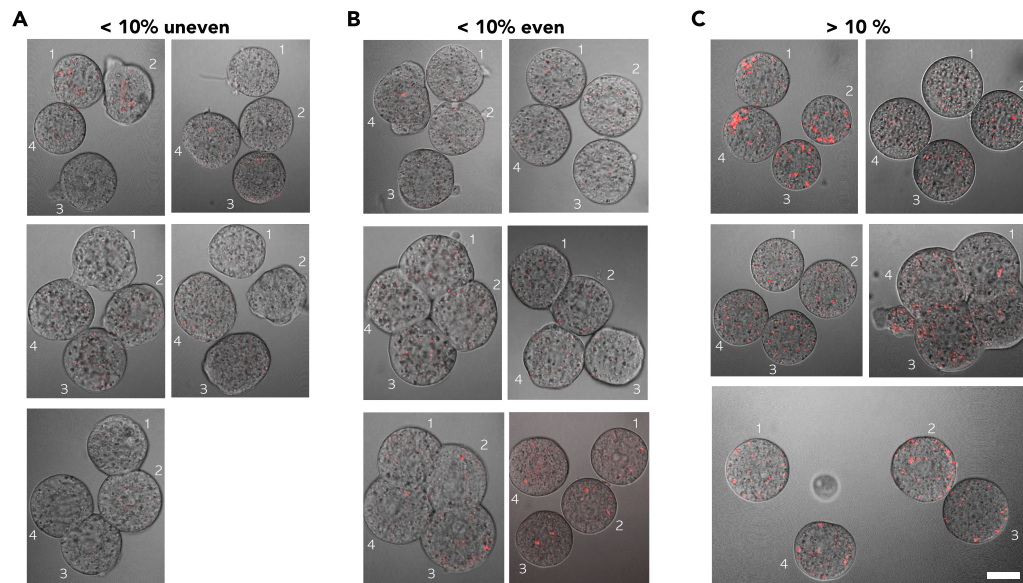


**Figure S4. Tracking donor mtDNA distribution in embryos at 4-cell stage,** Related to Figure 4 (A) Uneven distribution of donor mtDNA in embryos at 4-cell stage from heteroplasmic oocytes with <10% donor mtDNA. (B) Even distribution of donor mtDNA in embryos at 4-cell stage from heteroplasmic oocytes with <10% donor mtDNA. (C) Even distribution of donor mtDNA in embryos at 4-cell stage from heteroplasmic oocytes with >10% donor mtDNA. Scale bar, 40  $\mu\text{m}$ .

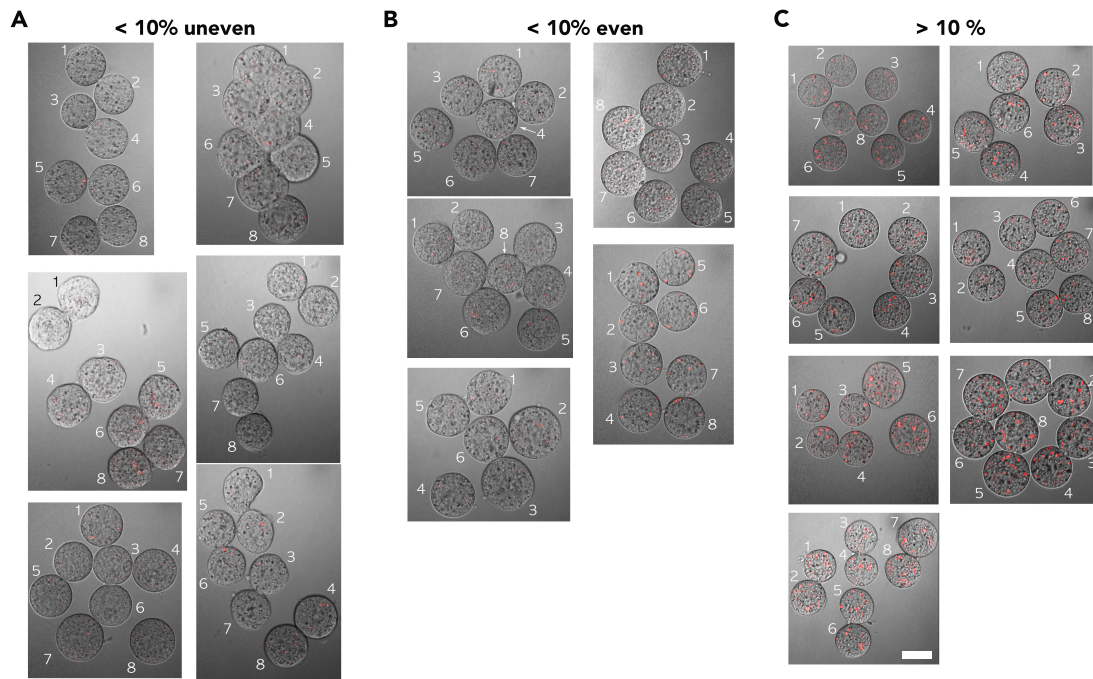


**Figure S5. Tracking donor mtDNA distribution in embryos at 8-cell stage,** Related to Figure 4  
 (A) Uneven distribution of donor mtDNA in embryos at 8-cell stage from heteroplasmic oocytes with <10% donor mtDNA. (B) Even distribution of donor mtDNA in embryos at 8-cell stage from heteroplasmic oocytes with <10% donor mtDNA. (C) Even distribution of donor mtDNA in embryos at 8-cell stage from heteroplasmic oocytes with >10% donor mtDNA. Scale bar, 40  $\mu$ m.

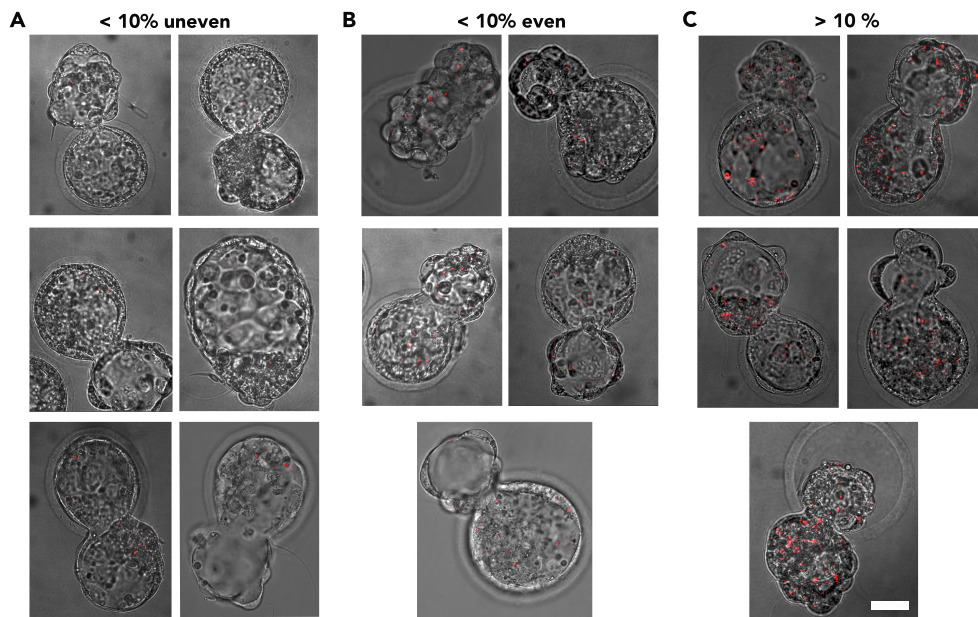


**Figure S6. Tracking donor mtDNA distribution in blastocysts, Related to Figure 4**  
 (A) Uneven distribution of donor mtDNA in blastocysts from heteroplasmic oocytes with <10% donor mtDNA. (B) Even distribution of donor mtDNA in blastocysts from heteroplasmic oocytes with <10% donor mtDNA. (C) Even distribution of donor mtDNA in blastocysts from heteroplasmic oocytes with >10% donor mtDNA. The fourth image in (A) and the second image in (C) (count by row) was also presented in Figure 4B to demonstrate the living cell staining experiment. Scale bar, 40  $\mu$ m.

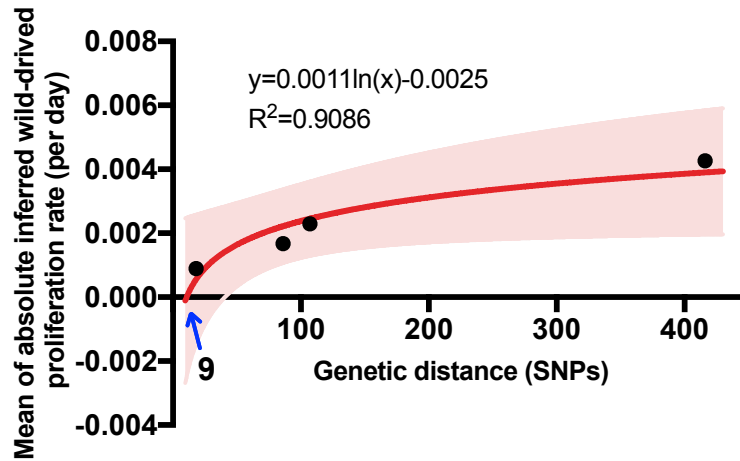


**Figure S7. Correlation of proliferation rate of wild-derived mtDNA and genetic distance,**  
 Related to Figures 1-4.

The proliferation rate increases as genetic distance of haplotypes rises based on past data (Burgstaller et al., 2014). When the genetic distance is less than 9 SNPs, the anticipated mean of proliferation rate equals to 0. Regression curve and shaded region (red) show curve model fit and 95% confidence intervals.



## Supplemental Tables

**Table S1. Nucleotide differences between B6D2F1(C57/BL6×DBA) and NZW/Lac J mitochondrial DNA, Related to Figures 1, 2 and Transparent Methods.**

Genes	Polymorphism	Sequences
<b>ND3</b>	C9461T	Query 9421 TCCAATTAGTAGATTCTGAATAAACCCAGAAGAGAGTAATCAACCTGTACACTGTTATCT 9480 Sbjct 9421 TCCAATTAGTAGATTCTGAATAAACCCAGAAGAGAGTAATTAAACCTGTACACTGTTATCT 9480
<b>tRNA-Arg</b>	A9821-	Query 9781 AAAAAGGATTAGAATGAACAGAGTAAATGGTAATTAGTTTAAAAAAAATTAATGATTTC 9840 Sbjct 9781 AAAAAGGATTAGAATGAACAGAGTAAATGGTAATTAGTTTAAAAAAAATTAATGATTTC 9839
<b>ND5</b>	C13053T	Query 13021 ATTTACTTCGTAACAATAACAAAACCGCGTTTCCCCCCTAATCTCCATTACGAAAAT 13080 Sbjct 13020 ATTTACTTCGTAACAATAACAAAACCGCGTTTCCCCCCTAATCTCCATTACGAAAAT 13079

**Table S2. Primer sequences and conditions of PCR for mitochondria genome (nucleotide position, 9201-11102) amplification, Related to Figures 1, 2 and Transparent Methods.**

Primary PCR	5'-ATGGCTACTGGATTCCATGG-3' 3'- GCTCCTATGAAGCTTCATGG-5'
Conditions	95°C for 3 min; 40 cycles with denaturation at 94°C for 30 s, annealing at 59°C for 30 s, and elongation at 72°C for 1 min; 1 cycle at 72°C for 7 min; hold at 4°C
Second round PCR	5'-TTTGAAGCCGCAGCATGA-3' 3'-ATTTATTTGGGGGAGTCAGAATGC-5'
Conditions	95°C for 3 min, 40 cycles with denaturation at 94°C for 30 s, annealing at 53°C for 30 s, and elongation at 72°C for 1 min; 1 cycle at 72°C for 7 min; hold at 4°C

**Table S3. Heteroplasmy in adult tissues, Related to Figures 1 and 3.**

Mouse	Donor mtDNA (%) in adult tissues															Mean (%)	S.D.	V'(h)	Range (%)
	Brain	Heart	Lung	Liver	Kidney	Stomach	Intestine	Spleen	Muscle	Adipose	Skeleton	Bladder	Gonad	Hypoth-alamus	Optic Nerve	Skin			
1	0	2.71	0	3.15	0	3.66	0	0	0	3.81	0	2.2	2.88	0	0	11.29	1.86	0.03	0.0478
2	6.21	0	6.49	0	0	0	7.16	4.45	2.9	5.66	0	6.36	0	6.96	0	6.13	3.27	0.03	0.0311
3	0	6.6	4.43	6.13	4.62	6.15	4.32	5.23	4.77	6.6	4.57	5.91	5.44	5.13	6.26	0	4.76	0.02	0.0089
4	7.67	0	7.58	0	7.69	0	7.29	5.63	4.95	7.05	6.73	7.33	4.94	7.4	5.68	5.96	5.37	0.03	0.0156
5	7.32	7.02	0	0	8.02	6.97	9.17	5.43	8.49	8.11	7.68	7.22	5.17	7.81	5.28	7.11	6.30	0.03	0.0124
6	5.58	6.28	4.62	6.43	7.56	7.05	6.12	6.3	6.6	6.14	7.04	5.89	6.06	6.32	6.13	6.78	6.31	0.01	0.0008
7	8.67	0	8.13	0	8.52	5.48	8.46	6.29	6.53	8.33	6.29	9.16	6.04	9.17	6.48	7.1	6.54	0.03	0.0130
8	6.85	6.65	6.16	6.28	6.89	5.48	6.18	7.58	5.91	7.28	6.77	7.19	6.73	6.58	8.19	6.87	6.72	0.01	0.0007
9	5.62	8.73	6.6	7.61	7.4	7.16	0	0	9.31	6.29	9.08	7.05	9.71	8.53	7.94	7.32	6.77	0.03	0.0131
10	9.07	0	9.23	8.58	8.46	0	8.53	5.8	9.21	8.35	6.27	8.13	6.95	8.93	6.72	7.58	6.99	0.03	0.0132
11	9.37	5.94	8.8	5.91	8.77	5.49	6.89	6.2	7.43	7.48	6.67	8.69	4.88	7.91	5.93	8.35	7.17	0.01	0.0028
12	6.53	7.89	5.81	8.56	7.21	8.63	5.63	8.51	7.94	11.04	7.2	8.11	8.73	7.21	7.76	7.19	7.75	0.01	0.0023
13	7.58	9.7	6.43	7.9	8.68	6.52	8.74	6.35	9.68	6.29	9.02	8.42	8.77	8.31	8.41	10.18	8.19	0.01	0.0021
14	8.82	10.28	9.08	9.48	8.26	11.47	8.22	10.76	8.54	10.89	9.28	10.19	10.56	9.34	10.28	10.6	9.75	0.01	0.0012
15	8.43	9.96	9.71	10.82	9.89	12.35	12.96	10.85	10.3	11.35	11.71	7.87	9.74	9.48	10.14	1.94	9.84	0.02	0.0070
16	10.58	9.81	10.89	8.75	9.33	9.99	9.32	10.08	10.77	10.85	9.32	10.16	9.09	9.26	10.62	10.65	9.97	0.01	0.0006
17	11.18	9.47	10.08	9.77	11.23	7.82	12.68	9.84	9.12	11.67	11.06	12.06	7.85	11.26	8.82	13.08	10.44	0.02	0.0027
18	10.54	13.33	11.6	13.38	12.17	10.86	14.34	11.78	13.41	11.34	12.04	11.63	12.7	11.65	12.5	11.17	12.15	0.01	0.0010
19	12.06	12.18	11.75	14.36	12.68	11.25	14.81	12.56	12.96	12.88	14.03	11.03	15.03	14.6	13.02	10.21	12.84	0.01	0.0018

20	14.99	11.9	15.12	10.83	13.84	10.48	14.02	11.85	13.96	15.61	12.38	15.12	12.24	14.04	11.67	11.81	13.12	0.02	0.0024	5.13
21	15.19	14.63	13.61	10.79	14.4	9.61	13.89	12.5	13.28	12.68	12.6	13.14	12.45	14.42	13.62	16.36	13.32	0.02	0.0023	6.75
22	13.71	13.37	14.69	12.46	15.19	11.97	14.43	13.72	11.95	13.86	12.29	15.03	11.18	15.74	11.94	14.39	13.50	0.01	0.0016	4.56
23	15.68	14.45	15.66	11.47	15.34	13.22	15.58	14.37	16.69	15.71	14.79	16.49	15.4	16.45	13.24	17.09	15.10	0.01	0.0017	5.62
24	14.23	16	15	16.38	14.87	13.33	14.71	12.37	15.47	13.16	16.76	15.46	17.76	15.68	15.51	16.67	15.21	0.01	0.0016	5.39
25	15.32	15.9	14.48	14	14.42	17.34	14.56	15.57	13.92	15.38	15.45	16.69	16.9	14.66	15.21	15.33	15.32	0.01	0.0008	3.42
26	14.93	16.68	14.36	13.73	16.79	15.9	15.03	15.74	17.14	14.6	16.85	15.46	16.89	15.89	17.32	15.06	15.77	0.01	0.0009	3.59
27	16.62	19.69	17.74	16.46	17.53	17.68	18.92	17.33	17.25	17.58	19.03	18.98	19.02	19.93	18.37	16.93	18.07	0.01	0.0008	3.47
28	21.24	20.76	23.06	17.67	20.71	21.88	23.19	19.06	19.14	20.73	20.38	19.76	18.42	21.38	18.55	21.9	20.49	0.02	0.0016	5.52
29	19.91	21.99	21.29	23.08	23.94	18.38	25.25	20.39	21.26	19.3	22.02	21.65	22.76	21.75	23.28	15.81	21.38	0.02	0.0031	9.44
30	21.58	21.38	22.58	20.83	20.44	21.63	21.66	22.1	21.87	23.86	21.4	22.56	22.55	19.13	21.87	21.94	21.71	0.01	0.0006	4.73
31	23.64	25.23	24.62	22.35	25.8	24.68	24.42	23.84	26.53	24.86	21.92	23	24	21.78	24.7	17.87	23.70	0.02	0.0023	8.66
32	24.14	24.22	26.75	22.79	27.03	23.91	24.93	22.59	25.19	23.52	23.06	23.22	21.92	24.1	22.02	25.26	24.04	0.02	0.0012	5.11
33	24.3	27.65	25.87	26.5	26.72	23.97	24.95	24.48	23.23	24.86	24.11	24.01	24.44	21.89	23.68	22.48	24.57	0.02	0.0013	5.76
34	27.33	27.69	26.11	25.77	29.92	28.17	27.99	26.05	27.02	25.81	25.35	26.32	23.94	28.21	26.55	26.04	26.77	0.01	0.0010	5.98
35	32.54	33.41	31.53	34.13	32.01	34	32.58	33.91	32.94	28.67	33.46	33.89	33.49	32.36	33.82	35.58	33.02	0.02	0.0010	6.91
36	35.71	33.56	33.57	32.39	36.79	32.72	36.72	32.23	36.15	32.31	36.23	36.85	35.31	34.27	36.31	34.81	34.75	0.02	0.0013	4.62
37	39.3	40	37.37	40.72	35.73	41.9	36.39	39.04	33.79	37.16	36.58	39.05	39.28	39.01	38.91	35.91	38.13	0.02	0.0019	8.11
Mean	14.39	14.19	14.35	13.50	14.83	13.71	14.87	13.80	14.48	14.62	14.31	14.90	14.30	14.77	14.24	14.34	14.35	0.02	0.0056	6.01

S.D., standard deviation; V'(h), normalised variance; Range, differences between maximum and minimum values among 16 adult tissues.

**Table S4. Heteroplasmy in blastomeres of 2 cell embryos, Related to Figures 2 and 3.**

Embryo	Donor mtDNA (%) in blastomeres		Mean (%)	S.D.	V'(h)	Range (%)
	1	2				
1	3.89	0.00	1.95	0.02	0.0198	3.89
2	5.86	0.00	2.93	0.03	0.0302	5.86
3	6.04	0.00	3.02	0.03	0.0311	6.04
4	2.23	4.71	3.47	0.01	0.0046	2.48
5	4.16	4.92	4.54	0.00	0.0003	0.76
6	8.74	6.08	7.41	0.01	0.0026	2.66
7	5.58	9.97	7.78	0.02	0.0067	4.39
8	9.52	10.05	9.79	0.00	0.0001	0.53
9	10.93	8.79	9.86	0.01	0.0013	2.14
10	8.79	12.53	10.66	0.02	0.0037	3.74
11	15.39	15.39	15.39	0.00	0.0000	0.00
12	14.88	16.09	15.49	0.01	0.0003	1.21
13	15.24	15.91	15.58	0.00	0.0001	0.67
14	16.85	14.45	15.65	0.01	0.0011	2.40
15	23.41	8.91	16.16	0.07	0.0388	14.50
16	18.66	16.38	17.52	0.01	0.0009	2.28
17	18.99	16.74	17.87	0.01	0.0009	2.25
18	19.88	20.58	20.23	0.00	0.0001	0.70
19	23.05	20.56	21.81	0.01	0.0009	2.49
20	23.05	20.56	21.81	0.01	0.0009	2.49
21	21.80	26.14	23.97	0.02	0.0026	4.34
22	26.86	24.23	25.55	0.01	0.0009	2.63
23	25.22	27.33	26.28	0.01	0.0006	2.11
24	27.84	28.06	27.95	0.00	0.0000	0.22
25	29.10	28.52	28.81	0.00	0.0000	0.58
26	37.43	41.82	39.63	0.02	0.0020	4.39

S.D., standard deviation; V'(h), normalised variance; Range, differences between maximum and minimum values in daughter blastomeres.

**Table S5. Heteroplasmy in blastomeres of 3-4 cell embryos, Related to Figures 2 and 3.**

Embryo	Donor mtDNA (%) in blastomeres				Mean (%)	S.D.	V'(h)	Range (%)
	1	2	3	4				
1	0.00	3.71	0.00	3.51	1.81	0.02	0.0184	3.71
2	3.99	0.00	3.24	0.00	1.81	0.02	0.0188	3.99
3	0.00	3.85	0.00	3.53	1.85	0.02	0.0189	3.85
4	3.12	0.00	4.86	0.00	2.00	0.02	0.0223	4.86
5	4.86	0.00	3.77	0.00	2.16	0.02	0.0228	4.86
6	5.69	0.00	0.00	4.63	2.58	0.03	0.0270	5.69
7	9.21	0.00	0.00	2.14	2.84	0.04	0.0519	9.21
8	6.17	0.00	5.55	0.00	2.93	0.03	0.0304	6.17
9	3.88	3.16	3.55	3.20	3.45	0.00	0.0003	0.72
10	5.51	4.77	5.08	0.00	3.84	0.02	0.0135	5.51
11	5.21	0.00	3.93	6.60	3.94	0.02	0.0160	6.60
12	4.51	4.18	4.06	5.50	4.56	0.01	0.0007	1.44
13	7.41	5.60	6.74	0.00	4.94	0.03	0.0182	7.41
14	6.95	6.91	7.88	5.21	6.74	0.01	0.0015	2.67
15	4.42	12.00	5.24	8.14	7.45	0.03	0.0128	7.58
16	11.46	9.68	12.70	0.00	8.46	0.05	0.0323	12.70
17	8.60	9.67	6.65	9.55	8.62	0.01	0.0019	3.02
18	9.83	7.41	9.66	8.82	8.93	0.01	0.0011	2.42
19	8.39	10.72	7.60	11.50	9.55	0.02	0.0030	3.90
20	11.25	10.20	8.54	8.50	9.62	0.01	0.0016	2.75
21	12.13	7.29	10.46	9.81	9.92	0.02	0.0034	4.84
22	10.52	8.07	11.72	10.98	10.32	0.01	0.0020	3.65
23	11.52	8.90	12.15	9.32	10.47	0.01	0.0021	3.25
24	12.65	14.00	9.52	9.75	11.48	0.02	0.0036	4.48
25	10.99	12.21	12.29	11.44	11.73	0.01	0.0003	1.30
26	13.98	13.94	11.81	NA	13.24	0.01	0.0009	2.17
27	14.95	10.79	14.14	14.86	13.69	0.02	0.0024	4.16
28	13.14	13.76	15.16	15.08	14.29	0.01	0.0006	2.02
29	14.56	14.03	14.42	14.72	14.43	0.00	0.0001	0.69
30	14.51	14.77	14.88	NA	14.72	0.00	0.0000	0.37
31	9.94	16.07	17.84	15.91	14.94	0.03	0.0070	7.90

<b>32</b>	15.94	17.26	14.24	NA	15.81	0.01	0.0011	3.02
<b>33</b>	15.35	16.68	16.33	16.81	16.29	0.01	0.0002	1.46
<b>34</b>	19.22	16.09	15.85	18.64	17.45	0.01	0.0016	3.37
<b>35</b>	17.19	20.44	17.33	NA	18.32	0.02	0.0015	3.25
<b>36</b>	21.89	22.20	19.28	21.59	21.24	0.01	0.0008	2.92
<b>37</b>	21.59	23.76	20.86	24.63	22.71	0.02	0.0013	3.77
<b>38</b>	22.40	24.94	23.24	22.01	23.15	0.01	0.0007	2.93
<b>39</b>	27.86	24.13	25.89	29.14	26.76	0.02	0.0019	5.01
<b>40</b>	22.63	33.66	33.71	NA	30.00	0.05	0.0129	11.08
<b>41</b>	56.28	50.94	54.14	53.23	53.65	0.02	0.0015	5.34
<b>42</b>	54.39	50.12	55.90	56.53	54.24	0.02	0.0025	6.41

---

S.D, standard deviation; CV, coefficient of variation; Range, differences between maximum and minimum values in daughter blastomeres; NA, none applicable.

---

**Table S6. Heteroplasmy in blastomeres of 6-8 cell embryos, Related to Figures 2 and 3.**

Embryo	Donor mtDNA (%) in blastomeres								Mean (%)	S.D.	V'(h)	Range (%)
	1	2	3	4	5	6	7	8				
1	4.25	0	4.79	0	3.5	0	3.29	4.7	2.57	0.02	0.0167	4.79
2	4.54	8.83	0.00	6.90	0.00	3.21	0.00	1.90	3.17	0.03	0.0324	8.83
3	3.85	7.67	6.68	3.57	3.66	0	2.79	1.76	3.75	0.02	0.0149	7.67
4	0	0	0	3.81	7.46	8.7	5.59	5.08	3.83	0.03	0.0290	8.70
5	21.04	0	3.8	0	0	0	NA	NA	4.14	0.08	0.1488	21.04
6	0	0.00	0.00	2.97	0.00	3.10	3.17	39.83	6.13	0.13	0.2853	39.83
7	7.42	5.69	6.59	5.27	6.08	5.93	7.12	5.24	6.17	0.01	0.0010	2.18
8	10.92	0	7.34	0	11.78	5.69	8.24	8.19	6.52	0.04	0.0285	11.78
9	6.75	7.80	6.34	7.06	9.10	6.92	10.02	NA	7.71	0.01	0.0022	3.68
10	8.96	9.59	7.28	10.6	7.33	9.37	7.47	NA	8.66	0.01	0.0019	3.32
11	5.75	7.73	6.33	8.76	12.54	11.08	14.15	7.28	9.20	0.03	0.0098	8.40
12	7.11	9.21	12.77	12.97	5.15	11.98	NA	NA	9.87	0.03	0.0099	7.82
13	15.49	8.13	8.63	16.99	7.61	5.49	7.27	NA	9.94	0.04	0.0188	11.50
14	8.69	8.36	11.03	8.96	11.65	9.81	10.72	11.37	10.07	0.01	0.0016	3.29
15	18.62	20.95	11.41	6.55	5.59	5.11	NA	NA	11.37	0.06	0.0397	15.84
16	8.13	11.01	6.58	9.26	3.97	12.68	22.66	25.32	12.45	0.07	0.0467	21.35
17	13.95	12.35	12.82	13.84	13.76	12.99	12.32	12.34	13.05	0.01	0.0004	1.63
18	16.93	8.46	12.81	13.43	14.14	14.71	11.98	14.17	13.33	0.02	0.0045	8.47
19	12.84	15.03	17.72	16.17	14.37	16.07	15.32	21.30	16.10	0.02	0.0042	8.46
20	11.42	12.90	37.15	11.67	14.84	13.27	12.91	NA	16.31	0.09	0.0538	25.73
21	20.79	19.75	19.19	18.59	14.96	15.09	15.37	12.94	17.09	0.03	0.0050	7.85
22	17.46	15.58	16.81	16.18	17.81	19.19	NA	NA	17.17	0.01	0.0010	3.61
23	18.18	21.37	18.56	16.3	18.6	17.07	15.92	NA	18	0.02	0.0019	5.45
24	12.06	29.32	19.8	14.68	22.81	22.12	24.61	15.88	20.16	0.05	0.0178	17.26
25	21.16	27.53	20.11	22.74	23.09	22.51	20.3	28.19	23.20	0.03	0.0047	8.08
26	29.51	32.13	27.42	28.24	26.86	28.11	25.35	NA	28.23	0.02	0.0020	6.78
27	29.25	33.07	27.62	29.24	27.64	31.90	29.92	19.12	28.47	0.04	0.0077	13.95
28	33.84	38.34	34.65	34.17	36.28	34.54	35.97	37.34	35.64	0.02	0.0010	4.50
29	36.33	47.29	37.67	33.27	34	33.25	NA	NA	36.97	0.05	0.0103	14.04
30	35.13	34.98	37.57	36.67	39.36	37.55	38.19	NA	37.06	0.01	0.0009	4.38
31	47.09	37.87	41.8	38.35	42.21	44.99	39.29	NA	41.66	0.03	0.0042	9.22



<b>32</b>	49.7	41.29	50.21	44.04	46.5	44.37	45.76	NA	45.98	0.03	0.0035	8.92
<b>33</b>	51.34	50.6	51.45	51.56	52.15	54.36	NA	NA	51.91	0.01	0.0006	3.76

---

S.D, standard deviation; CV, coefficient of variation; Range, differences between maximum and minimum values in daughter blastomeres; NA, none applicable.

---

**Table S7. Fluorescence intensity in blastomeres of 2 cell embryos, Related to Figure 4.**

Proportion of mitotracker	Embryo	Fluorescence intensity in blastomeres		Proportion		Variance
		1	2	1	2	
<10% uneven	1	44770	7297	0.86	0.14	0.0198
	2	7302	3887	0.65	0.35	0.0302
	3	27181	0	1.00	0.00	0.0311
	4	170043	32531	0.84	0.16	0.0046
	5	76730	16188	0.83	0.17	0.0003
<10% even	1	35819	33211	0.52	0.48	0.0026
	2	29913	14320	0.68	0.32	0.0067
	3	17629	29768	0.37	0.63	0.0001
	4	54076	49367	0.52	0.48	0.0013
	5	30674	33145	0.48	0.52	0.0037
	6	92391	104795	0.47	0.53	0.0000
>10%	1	147731	106206	0.58	0.42	0.0003
	2	233691	174094	0.57	0.43	0.0001
	3	190303	260991	0.42	0.58	0.0011
	4	592428	338429	0.64	0.36	0.0388
	5	1422731	2361465	0.38	0.62	0.0009
	6	1359749	672487	0.67	0.33	0.0009

Proportion, the ratio of each blastomere fluorescence intensity to total intensity; variance, variance of proportion.

**Table S8. Fluorescence intensity in blastomeres of 4 cell embryos, Related to Figure 4.**

Proportion of mitotracker	Embryo	Fluorescence intensity in blastomeres				Proportion				Variance
		1	2	3	4	1	2	3	4	
<10% uneven	1	150041	128995	0	70537	0.43	0.37	0.00	0.20	0.0278
	2	8448	2662	66156	44323	0.07	0.02	0.54	0.36	0.0461
	3	25738	153750	181180	94722	0.06	0.34	0.40	0.21	0.0172
	4	4180	0	26384	41607	0.06	0.00	0.37	0.58	0.0548
	5	13082	57861	4806	3752	0.16	0.73	0.06	0.05	0.0782
<10% even	1	24502	38983	10516	69138	0.17	0.27	0.07	0.48	0.0230
	2	66231	44487	28675	41905	0.37	0.25	0.16	0.23	0.0055
	3	114208	44697	102938	39832	0.38	0.15	0.34	0.13	0.0123
	4	33237	46103	33116	42960	0.21	0.30	0.21	0.28	0.0014
	5	28904	48390	113791	39221	0.13	0.21	0.49	0.17	0.0208
	6	88670	107586	111489	95982	0.22	0.27	0.28	0.24	0.0005
>10%	1	590333	638842	579461	806561	0.23	0.24	0.22	0.31	0.0012
	2	335749	290522	267510	231713	0.30	0.26	0.24	0.21	0.0011
	3	232264	263602	290182	312649	0.21	0.24	0.26	0.28	0.0007
	4	185487	151531	414783	391565	0.16	0.13	0.36	0.34	0.0107
	5	648333	1015563	368786	522352	0.25	0.40	0.14	0.20	0.0088
Proportion, the ratio of each blastomere fluorescence intensity to total intensity; variance, variance of proportion.										

Table S9. Fluorescence intensity in blastomeres of 6-8 cell embryos, Related to Figure 4.																		
Proportion of mitotracker	Embryo	Fluorescence intensity in blastomeres								Proportion								Variance
		1	2	3	4	5	6	7	8	1	2	3	4	5	6	7	8	
<10% uneven	1	3039	3698	1537	9627	25819	8369	4377	1355	0.05	0.06	0.03	0.17	0.45	0.14	0.08	0.02	0.0171
	2	24950	1618	2611	28760	0	6518	1116	5436	0.35	0.02	0.04	0.41	0.00	0.09	0.02	0.08	0.0224
	3	0	0	10006	14533	73739	56436	7347	77209	0.00	0.00	0.04	0.06	0.31	0.24	0.03	0.32	0.0170
	4	14540	19066	7499	22147	13967	13924	0	0	0.16	0.21	0.08	0.24	0.15	0.15	0.00	0.00	0.0071
	5	40895	1619	3880	22006	6828	2726	11442	0	0.46	0.02	0.04	0.25	0.08	0.03	0.13	0.00	0.0213
	6	14468	50243	10369	39879	26394	45449	6960	24044	0.01	0.22	0.03	0.23	0.17	0.04	0.23	0.07	0.0082
<10% even	1	1636	38848	5745	40990	31144	6836	41016	12283	0.31	0.11	0.03	0.13	0.30	0.02	0.10	NA	0.0122
	2	34253	22860	44841	45996	11659	54296	20628	72583	0.11	0.07	0.15	0.15	0.04	0.18	0.07	0.24	0.0037
	3	36344	12701	3702	15010	34763	2107	10986	NA	0.16	0.11	0.09	0.04	0.08	0.17	0.12	0.22	0.0028
	4	34253	22860	44841	45996	11659	54296	20628	72583	0.14	0.36	0.07	0.12	0.16	0.16	NA	NA	0.0081
	5	32328	22743	18416	8944	16369	34701	23669	44728	0.16	0.10	0.12	0.10	0.20	0.11	0.11	0.11	0.0012
>10%	1	14012	35680	6909	12183	15539	15757	NA	NA	0.17	0.09	0.10	0.14	0.11	0.16	0.11	0.11	0.0007
	2	115035	68640	83185	75013	144522	77619	76613	75835	0.15	0.13	0.18	0.18	0.21	0.14	NA	NA	0.0009
	3	136937	76765	86675	115616	91588	134712	91084	94228	0.12	0.17	0.14	0.09	0.08	0.18	0.23	NA	0.0024
	4	178010	148108	210702	214750	249067	161807	NA	NA	0.14	0.08	0.11	0.13	0.14	0.11	0.18	0.09	0.0009
	5	133526	181106	153246	92104	81988	189512	241635	NA	0.13	0.11	0.08	0.10	0.32	0.26	NA	NA	0.0083
	6	101428	56838	80342	95025	97152	79724	128508	64966	0.11	0.14	0.10	0.09	0.17	0.07	0.17	0.14	0.0014
	7	118481	107027	75974	92444	305334	245952	NA	NA	0.13	0.15	0.09	0.11	0.12	0.09	0.13	0.19	0.0009

---

Proportion, the ratio of each blastomere fluorescence intensity to total intensity; variance, variance of proportion; NA, none applicable.

---

Table S10. Fluorescence intensity in regions of blastocyst, Related to Figure 4.

Proportion of mitotracker	embryo	Fluorescence intensity in regions of blastocyst										Proportion										Variance
		1	2	3	4	5	6	7	8	9	10	1	2	3	4	5	6	7	8	9	10	
<10% uneven	1	0	3419	0	0	0	0	0	0	0	0	0.00	1.00	0.00	0.00	0.00	0.00	0.00	0.00	0.00	0.00	0.0900
	2	0	5555	0	0	0	0	0	4592	4828	8172	0.00	0.24	0.00	0.00	0.00	0.00	0.00	0.20	0.21	0.35	0.0165
	3	0	0	0	0	0	2447	7167	0	0	0	0.00	0.00	0.00	0.00	0.00	0.25	0.75	0.00	0.00	0.00	0.0521
	4	0	0	7753	0	0	1188	0	0	9451	0	0.00	0.00	0.42	0.00	0.00	0.06	0.00	0.00	0.51	0.00	0.0346
	5	7223	5301	0	0	0	0	0	5918	22981	0	0.17	0.13	0.00	0.00	0.00	0.00	0.00	0.14	0.55	0.00	0.0275
	6	7756	0	0	3556	0	23785	0	0	0	0	0.22	0.00	0.00	0.10	0.00	0.68	0.00	0.00	0.00	0.00	0.0418
<10% even	1	12377	24569	44108	19765	2648	2444	5591	393	7186	0	0.10	0.21	0.37	0.17	0.02	0.02	0.05	0.00	0.06	0.00	0.0125
	2	7303	10915	16585	22295	6898	9332	6742	3854	0	0	0.09	0.13	0.20	0.27	0.08	0.11	0.08	0.05	0.00	0.00	0.0062
	3	23954	18478	0	10546	0	0	10900	7836	23400	2398	0.25	0.19	0.00	0.11	0.00	0.00	0.11	0.08	0.24	0.02	0.0085
	4	0	14054	9787	21325	3070	7415	7877	11165	6195	8866	0.00	0.16	0.11	0.24	0.03	0.08	0.09	0.12	0.07	0.10	0.0039
	5	0	0	20183	46521	1807	9458	0	6461	26690	21930	0.00	0.00	0.15	0.35	0.01	0.07	0.00	0.05	0.20	0.16	0.0120
>10%	1	14657	11743	27500	67664	124327	19723	22254	23700	14729	51855	0.04	0.03	0.07	0.18	0.33	0.05	0.06	0.06	0.04	0.14	0.0078
	2	90847	1925	26203	63079	54377	61617	74529	31476	62918	34358	0.18	0.00	0.05	0.13	0.11	0.12	0.15	0.06	0.13	0.07	0.0025
	3	32887	21227	24335	14613	40121	20612	69636	15484	46936	15639	0.11	0.07	0.08	0.05	0.13	0.07	0.23	0.05	0.16	0.05	0.0031
	4	19699	42001	6231	3064	13044	20212	8052	0	20484	2093	0.15	0.31	0.05	0.02	0.10	0.15	0.06	0.00	0.15	0.02	0.0080
	5	23139	20390	173049	186452	23889	1991	55685	18418	82425	59600	0.04	0.03	0.27	0.29	0.04	0.00	0.09	0.03	0.13	0.09	0.0092

Proportion, the ratio of each blastomere fluorescence intensity to total intensity; variance, variance of proportion.

## Transparent Methods

### Animals breeding scheme and ethics statement

Mitochondria replacement founders were generated from our lab between female NZW/LacJ (NZW) and female BDF1 from C57/BL6×DBA (C57) during the past study (Wang et al., 2014). Then the female founders were mated with male mice (BDF1) to reproduce heteroplasmic mice for this study. All mice used in this study were maintained in accordance with the guidelines of the Laboratory Animal Service, Fudan University (research license 20160225-103).

### Generation of heteroplasmic standard samples

Whole genomic DNA of C57 and NZW were extracted from liver. Then the region of mitochondria genome (nucleotide position, 9201-11102) was amplified using primers of primary PCR and condition in Table S2. PCR products were cloned using the pMD18-T Vector System (Takara) according to the manufacturer's instructions. Plasmid DNA was isolated using QIAGEN Plasmid Kit. The DNA concentration was determined by Quantitative real-time PCR using ViiA 7 Real-Time PCR System (Applied Biosystems) with primers of primary PCR and condition in Table S2. Equimolar concentrations of mtDNA with C57 and NZW genotypes were combined in varying ratios to generate gradient standard samples, ranging from 0 to 25%.

### Genotyping of donor mtDNA Heteroplasmy Level of embryonic blastomeres and adult tissues

Zona pellucida of embryos at 2-cell, 4-cell, and 8-cell stage was digested by brief exposure to 0.5% of pronase (Roche, 70229227), 37°C, 5min. Then blastomeres of the denuded embryos were disaggregated by brief exposure to trypsin-EDTA, 37°C, 5min. The single blastomere was lysed into a 0.2 ml PCR tube containing 4 µl of PBS. Add 3 µl buffer D2 and incubate at 65 °C for 10 min, followed by adding 3 µl stop solution. Then whole genomic DNA from single blastomere was amplified using REPLI-g Single Cell Kit (QIAGEN, 150345).

Whole genomic DNA of heteroplasmic mice (6~8 months old) were isolated using DNA extracted from brain, heart, lung, liver, spleen, bone, bladder, gonad, pituitary, skin, optic nerve, stomach, intestine, fat, muscle, and kidney using Genomic DNA Kit (Tiangen).

To determine the distribution of donor mtDNA in pre-implanted embryos and adult tissues, the region of mice mitochondria genome (nucleotide position, 9201-11102) was amplified from total genome of single blastomere and tissue using the primary PCR. The primer sequences and conditions were seen in Table S2. PCR was performed using ABI cycler. The SNP used for detecting heteroplasmy is m.9461C>T (Table S1) and confirmed by pyrosequencing. Detailed methods for pyrosequencing were processed according to the previously described methods (Wang et al., 2014). The second round PCR sequences and conditions were seen in Table S2. Single-stranded biotinylated PCR products were prepared for sequencing by Pyrosequencing Vacuum Prep Tool (Biotage AB) according the protocol of PyroMark Q96 ID platform (Qiagen). Primer used for pyrosequencing was 5'-GAATAAACCCAGAAGAGAGT-3'. Quantification of the donor mtDNA heteroplasmy level of variant m.9461C>T was performed using allele frequency quantification (AQ) function in PyroQ-AQ software (Wang et al., 2014). A standard curve was generated by linking expected heteroplasmy values and actual heteroplasmy values for the gradient standard samples.

### Mathematical analysis to predict the genetic distance related to segregation

The mathematical model was created to describe the relationship between the proliferation rate

of donor mtDNA (calculated as mean of absolute inferred wild-derived proliferation rate) and genetic distance based upon past data (Burgstaller et al., 2014a). Logarithmic fitting on their 4 sets of data was performed to get the following expression:

$$r(d)=\begin{cases} 0 & 0\leq d\leq 9 \\ 0.0011\ln(d)-0.0025 & d\geq 10 \end{cases}$$

$r$  was defined as the mean proliferation rate of donor mtDNA and  $d$  as the genetic distance (SNPs) of mtDNA between haplotypes. This model is used to find the maximum genetic distance before segregation bias takes effect and predict the proliferation rate at a certain genetic distance (Figure S7).

### **Heteroplasmic oocytes construction by spindle-chromosome complex transfer (spindle transfer)**

The lyophilized MitoTracker Red CMXRos (M7512, Life Technology) was dissolved in high-quality, anhydrous dimethylsulfoxide (DMSO) to a final concentration of 1 mM to prepare a stock solution. Then stock solution was diluted to 250nM concentration (working solution) in G1 medium. Donor mouse oocytes were dyed with 250nM MitoTracker. Then Spindle-chromosome complex with different amount of red mitochondria were transferred into enucleated oocyte containing unstained mitochondria (Wang et al., 2014). All manipulations were performed on a 37 °C -heated stage (Tokai Hit) of a Nikon TE 2000S inverted microscope equipped with Narishige micromanipulators, a laser objective and an Oosight™ Imaging System. Stained oocytes and unstained oocytes were placed into manipulation droplets of G-gamete containing CB in a glass-bottom dish.

An unstained oocyte was suctioned with the holding pipette, so that the spindle was located in the 3 o'clock position. The zona pellucida close to the spindle was drilled with a laser, and an enucleation pipette was then inserted through the hole in the zona pellucida. The spindle was enucleated with a minimal amount of red mitochondria, and the enucleated oocyte was released into manipulation medium. Then the spindle-chromosome complex of stained oocyte was enucleated as the same to the unstained oocyte with a diameter of 12 μm pipette and then transferred to the HVJ-E (inactivated Hemagglutinating Virus of Japan envelope, GenomeOne, Cosmo Bio) drop for brief exposure. The enucleated spindle-chromosome complex (red) was slowly moved to the end of the pipette and a suction force was made to take up a small amount of HVJ-E into the pipette. The recipient oocyte was immobilized so that the drilled hole of the zona was at 3 o'clock position. The red spindle-chromosome complex was gently released from the pipette and transferred into the enucleated recipient oocyte. After that, the reconstructed oocytes were briefly left in the manipulation drop to allow the fusion of the red spindle-chromosome complex and the recipient oocyte for 10-20 min. After fusion, the reconstructed oocytes were washed several times and placed in HTF medium for recovery and *in vitro* fertilization. See also Video S1.

### **In Vitro Fertilization and culture after spindle transfer**

Male mice (BDF1, 10–15 weeks) were sacrificed by cervical dislocation. After dissections, sperms were incubated for sperm capacitation in HTF medium at 37.5°C under 5% CO<sub>2</sub>, 5% O<sub>2</sub>, incubation for 1 h. Then 2 × 10<sup>6</sup> sperms/ml were added into the HTF drops containing the heteroplasmic oocytes after spindle transfer. The sperms and heteroplasmic oocytes were co-cultured at 37.5°C for at least 4~6 hrs. Then heteroplasmic oocytes were washed three times in G1 medium. Oocytes with two visible pronuclei (2PN) were considered fertilized and transferred into G1 medium (100 μl drop) and cultured up to 72 hours at 37.5 °C under 5% CO<sub>2</sub>,



5% O<sub>2</sub>, and 90% N<sub>2</sub> incubation.

### **Living cell imaging of the whole embryos and its single blastomere developed from heteroplasmic oocytes**

To visualize the distribution of foreign mitochondria upon division, embryos developed from heteroplasmy oocytes were transferred to a 35mm glass bottom dish for mitoTracker analysis (Leica Microsystems, Inc.). Fluorescent images were obtained at 5-µm Z-axis intervals under confocal microscope.

To quantify and explore the distribution of stained mitochondria in daughter blastomeres, blastomeres of the reconstructed embryos were disaggregated by brief exposure to 0.5% pronase and 0.05% trypsin-EDTA. Then all blastomeres of a whole embryo were transferred to a 35mm glass bottom dish for analyzing distribution of stained mitochondria. Fluorescent images were obtained at 2-µm Z-axis intervals under confocal microscope. The relative fluorescent signals of blastomeres were determined using the Leica Application Suite-Advanced Fluorescence software.

### **Statistical Analysis**

Statistical analysis of mtDNA segregation was performed using GraphPad Prism 7. The normalised measure of heteroplasmy variance ( $V'(h)$ ) was used to compare heteroplasmy variance among samples with different mean heteroplasmy, taking the form

$$V'(h) = \frac{V(h)}{E(h)(1 - E(h))}$$

where  $V(h)$  is the variance of a set of samples and  $E(h)$  is its mean (Johnston et al., 2015, Johnston and Jones, 2016). To access donor mtDNA heteroplasmy in different tissues, Friedman test was used, where the significance was set at  $p < 0.05$ . For heteroplasmy level of three germ layers, Mann-Whitney test was performed, where the significance was set at  $p < 0.05$ . For correlation between heteroplasmy value and  $V'(h)$ , Spearman correlation test was used, where the significance was set at  $p < 0.05$ . For spread range of heteroplasmy value, Mann-Whitney test was employed, where the significance was set at  $p < 0.05$ . To access  $V'(h)$  of different development stages, Mann-Whitney test was performed, where the significance was set at  $p < 0.05$ . For heteroplasmy level of different development stages, Mann-Whitney test was used, where the significance was set at  $p < 0.05$ . For heteroplasmy value distribution, Kolmogorov-Smirnov test was performed, where the significance was set at  $p < 0.05$ . To access variance of fluorescence intensity in blastomeres, Mann-Whitney test was employed, where the significance was set at  $p < 0.05$ . Asterisks indicate statistical significance (\* denotes a p value of  $< 0.05$  and \*\* denotes a p value of  $< 0.01$ ).